

Investigation of a deep ice core from the Elbrus Western Plateau, the Caucasus, Russia

V. Mikhailenko¹, S. Sokratov², S. Kutuzov¹, P. Ginot^{3,7}, M. Legrand³, S. Preunkert³, I. Lavrentiev¹, A. Kozachek⁴, A. Ekaykin^{4,6}, X. Faïn³, S. Lim³, U. Schotterer^{5,a}, V. Lipenkov⁴, and P. Toropov^{1,8}

¹Institute of Geography, Russian Academy of Sciences, Moscow, Russia

²Arctic Environment Laboratory, Faculty of Geography, Lomonosov Moscow State University, Moscow, Russia

³Univ. Grenoble Alpes, CNRS – UMR5183, Laboratoire de Glaciologie et Géophysique de l'Environnement (LGGE), Grenoble, France

⁴Arctic and Antarctic Research Institute, St. Petersburg, Russia

⁵Climate and Environmental Physics Group, University of Bern, Bern, Switzerland

⁶St. Petersburg State University, St. Petersburg, Russia

⁷Observatoire des Sciences de l'Univers de Grenoble, IRD UMS222, CNRS, Université Joseph Fourier Grenoble 1, Saint Martin d'Hères, France

⁸Department of Meteorology and Climatology, Faculty of Geography, Lomonosov Moscow State University, Moscow, Russia

^a Retired

Correspondence to: V. Mikhailenko (mikhailenko@hotmail.com)

Abstract

A 182 meter ice core has been recovered from a borehole drilled through the glacier to the bedrock at the Western Plateau of Mt. Elbrus (43°20'53.9" N, 42°25'36.0" E; 5115 m a.s.l.), the Caucasus, Russia, in 2009. This is the first ice core in the region which represents a paleoclimate record practically undisturbed by seasonal melting. Relatively high snow accumulation rate at the drilling site enabled analysis of the intra-seasonal climate proxies' variability. Borehole temperatures ranged from -17 °C at 10 meters depth and -2.4 °C at 182 m. A detailed radio-echo sounding survey showed that the glacier thickness ranged from 45 meters near marginal zone of the plateau up to 255 m at the central part. The ice core has been analyzed for stable isotopes ($\delta^{18}\text{O}$ and δD), major ions (K^+ , Na^+ , Ca^{2+} , Mg^{2+} , NH_4^+ , SO_4^{2-} , NO_3^- , Cl^- , F^-), succinic acid ($\text{HOOCCH}_2\text{COOH}$), and tritium content. The mean annual net accumulation rate was estimated from distinct annual oscillations of $\delta^{18}\text{O}$, δD , succinic acid, and NH_4^+ and is 1455 mm w.e. for the last 140 years. Using annual layer counting also for the dating of the ice core, a good agreement with the absolute markers of the tritium 1963 bomb test time horizon located at the core depth of 50.7 m w.e. and the sulfate peak of the Katmai eruption (1912) at 87.7 m w.e. was obtained. According to mathematical modeling results, the

42 bottom ice age at the maximal glacier depth is predicted to be about 660 years BP. As the
43 2009 borehole was situated downstream of this point, the estimated bottom ice age of the
44 drilling site does not exceed 350–400 years BP. Taking into account the information that we
45 have acquired on the Western Plateau Elbrus glacier and first results of the ice core analysis,
46 these data can be used to reconstruct the atmospheric history of the European region.

47

48 **1 Introduction**

49

50 Climate and environmental changes, regional patterns, origin, and prediction are currently
51 among the most important scientific challenges. The functioning of the Earth's climate system
52 has a profound influence on society's development and human prosperity. The discrimination
53 of human-induced and natural climate variability is one of the most urgent tasks and it cannot
54 be solved using only short instrumental meteorological or atmospheric observations and
55 climate-chemistry modeling experiments. Proxy records (lake and marine sediments, ice
56 cores, tree rings, corals) can be used to substitute to some extent the instrumental climatic
57 records. Proxies can reach annual and seasonal resolution, and are useful as large networks
58 covering the areas of continental and even global scale. They can be calibrated against the
59 instrumental data. Such time series are appropriate for the statistical analyses and numerical
60 modeling. At this stage of development of modern paleoclimatology it is essential to have
61 reliable regional reconstructions for the last millennia (Vaughan et al., 2013). The study of
62 chemical impurities in cold glaciers snow and ice permit to reconstruct our changing
63 atmosphere from pre-industrial era to present-day (see Legrand and Mayewski, 1997 for a
64 review).

65 Ice cores from Polar glaciers (long-term-period of preservation and minimal disturbance
66 by melt/refreeze processes) are presently considered to be the best representation of the paleo-
67 climate and paleoenvironments at hemispheric scales. However, calculations based on
68 observational data trends in the major climatic characteristics show highly pronounced
69 regional variability. Such variability is reproduced by modern climate models and can be
70 projected into the future (AMAP, 2011), but the reliability of the simulations depends on the
71 amount and the quality of existent data and the results are questionable especially for the
72 precipitation rate (Anisimov and Zhil'tsova, 2012).

73 The need for longer glacier and paleoclimate records has led to the development of
74 numerous reconstructions of annual and seasonal resolution based on instrumental climate
75 data and paleoclimatic proxies. Ice cores from non-polar high mountain glaciers have been
76 used for reconstructing past atmospheric conditions. A number of studies examined climate

77 and environmental changes in various nonpolar areas (Vimeux et al., 2009; Thompson, 2010)
78 including the European Alps (Barbante et al., 2004; Preunkert and Legrand, 2013;
79 Schwikowski, 2004), the continental Siberian Altai (Eichler et al., 2011), and Kamchatka
80 (Kawamura et al., 2012; Sato et al., 2014).

81 Evidently, the best representation of the climate variability in a region of interest would
82 be from the region itself. Despite the temporal length of the records, the Greenland and the
83 Antarctic ice core data, though not disturbed by melting, is from sites which are very remote
84 from most of the inhabited areas. Therefore, the comparable paleo-climate records derived
85 directly from the glaciers in Europe and Asia are highly valuable. The problem is that the
86 seasonal melting and the water infiltration distort the climate proxies held in firn and ice even
87 at high altitudes of the Andes (Ginot et al., 2010), Himalaya (Hou et al., 2013) and low
88 latitudes of the Arctic islands (Kotlyakov et al., 2004).

89 The documented conditions (Tushinskii, 1968; Mikhalenko, 2008) near the top of Mt. Elbrus
90 allowed expectation of a reasonably long climatic record in an ice core not affected by melt
91 water infiltration. Relatively high accumulation rate at the site (Mikhalenko et al., 2005)
92 promised a high temporal resolution of the ice core data, apparently showing the seasonality
93 effect on the results of analysis (Werner et al., 2000). Interest to recover records from such
94 natural archive that preserve environmental data associated with atmospheric chemistry, dust
95 deposition, biomass burning, anthropogenic emission and climate change in the Caucasus
96 became a motivation for organizing the drilling campaign at the Western Plateau of Mt.
97 Elbrus (Mikhalenko, 2010). The aim of the Elbrus drilling project is climatic and
98 environmental reconstruction for Caucasian region from the ice core. After giving an
99 overview of the existing geographical, glaciological, meteorological, and climatological
100 knowledge already gained in the past from this region, this paper focuses on the glaciological
101 and glacio-chemical characterization of a new drilling site located on the Western Plateau of
102 Mt. Elbrus. A chronology for a 182 m depth ice core retrieved from this site is elaborated by
103 taking advantage benefit of stable isotopes and glacio-chemical records, as well as a
104 simplified thermo mechanically coupled modeling. Finally, an outlook on the possibilities to
105 develop the high-resolution regional paleoclimate reconstruction with this ice core is given.

106

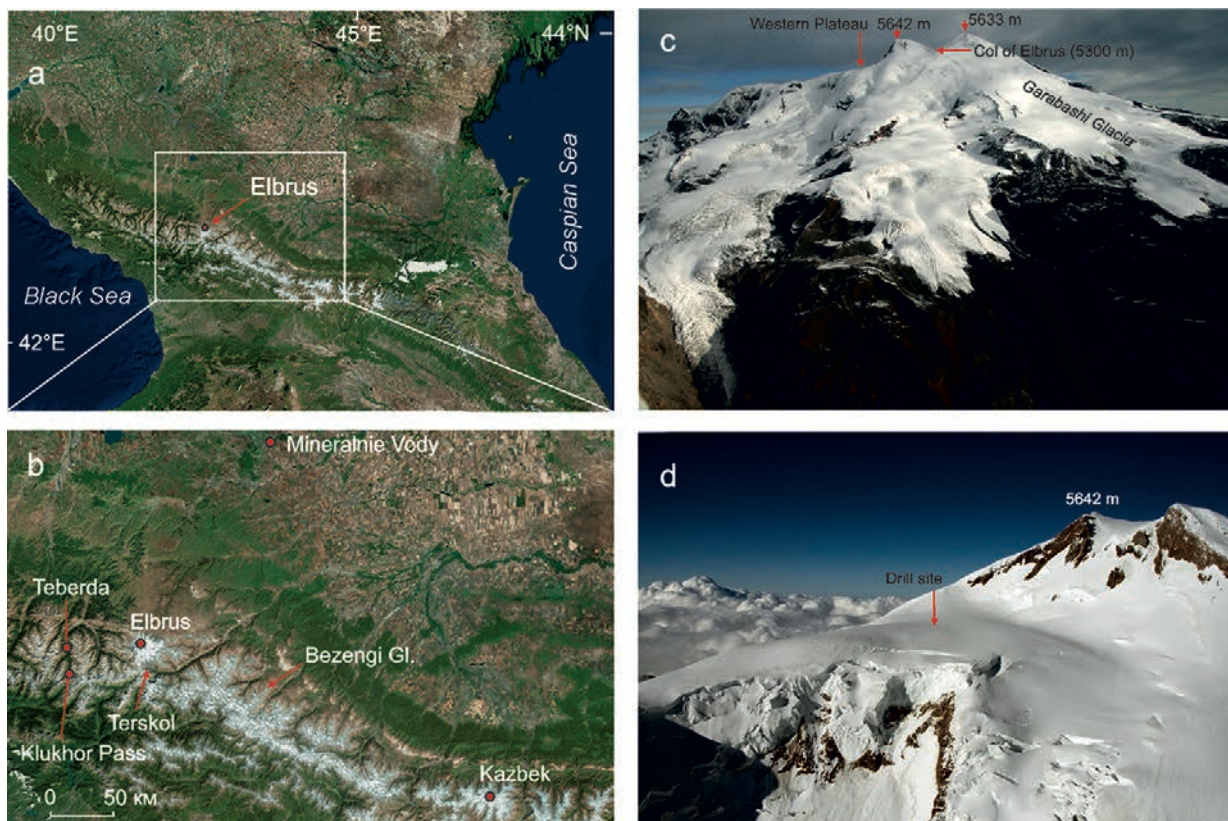
107 **2 Previous investigations of the Caucasus and the Mount Elbrus**

108

109 **2.1 Geographical and glaciological characteristics of the Caucasus region**

110

111 The Caucasus Mountains are situated between the Black and the Caspian seas, and are
 112 generally trending east-southeast, with the Greater Caucasus range often considered as the
 113 divide between Europe and Asia. The glaciers in the Caucasus cover an area of around
 114 $1121\pm 30 \text{ km}^2$ (Kutuzov et al., 2015) (Fig. 1).



115
 116 Figure 1. Location of study area: (a) – location of Mt. Elbrus in the Caucasus; (b) – location
 117 of glaciers and meteorological stations; (c) – Mt. Elbrus from the south with position of
 118 Western Plateau shown; (d) – Western Elbrus Plateau with drill site shown (photos by I.
 119 Lavrentiev on September 2009). ArcGIS World Imagery basemap used as a background.
 120 Source: DigitalGlobe.

121
 122 Glacier studies in the Caucasus were begun more than hundred years ago. They were
 123 mainly focused on glacier mapping (Pastukhov, 1893; Podozerski, 1911) and reconstruction
 124 of glacier position by geomorphological methods (Abich, 1875; Mushketov, 1882; Kovalev,
 125 1961; Serebryanny at el., 1984). Records of contemporary glaciological processes were
 126 obtained during the International Geophysical Year (IGY) in 1957–1959 (Tushinskii, 1968)
 127 when the climatic conditions of the glacial zone, accumulation and ablation of the glaciers,
 128 glacier runoff, glacier ice formation zones, and snow and firn stratigraphy were investigated.
 129 These studies have been conducted mainly on the southern slope of the Mt. Elbrus from the
 130 glacier tongues to the summits (see Figure 1b). It has been found that surface snow melting
 131 did not occur above 5000 m (Troshkina, 1968). Complex studies of mass, water, and heat

132 balances of glaciers in the Caucasus were started during the International Hydrological
133 Decade (1964–1974) (Golubev et al., 1978; Dyurgerov and Popovnin, 1988; Krenke et al.,
134 1988). A number of studies examined fluctuations of glacier dimensions and volume (Stokes
135 et al., 2006; Kutuzov et al., 2012, 2015; Nosenko et al., 2013, Shahgedanova et al., 2014),
136 glacier mass balance (Rototaeva and Tarasova, 2000) and regional snow chemistry (Kerimov
137 et al., 2011). Characteristics of the mineral dust and its source were investigated using shallow
138 ice cores and snow pits records from Mt. Elbrus (Kutuzov et al., 2013; Shahgedanova et al.,
139 2013).

140 There is a number of tree-ring based reconstructions representing mean summer air
141 temperature, river run-off and glacier mass balance in the region (Dolgova et al., 2013;
142 Solomina et al., 2012). First lake sediment cores retrieved in 2010, 2012 and 2013 did show a
143 good perspective in using lacustrine records to study long-term climate and glacier history
144 variations (Solomina et al., 2013).

145 Despite the substantial glacier area in the Caucasus, there is a very limited number of
146 suitable sites for ice core research due to relatively low elevation and considerable melting.
147 High-elevation vast flat parts of the glaciers of Elbrus (5642 m), Kazbek (5033 m), and
148 Bezengi (~5000 m) (see Fig. 1b) are the most promising sites for getting ice-core records.
149 Several shallow and intermediate depth ice cores have been recovered at the Caucasus
150 glaciers (Golubev et al., 1988; Zagorodnov et al., 1992; Bazhev et al., 1998), but they were
151 carried out at sites where considerable melt water percolation smoothed isotopic and
152 geochemical profiles.

153

154 **2.2 Geographical and glaciological characteristics of Mount Elbrus**

155

156 Mt. Elbrus, the highest summit of the Caucasus, consists in its upper part from two peaks –
157 the eastern (5621 m a.s.l.) and the western (5642 m a.s.l.) and is covered by glaciers with total
158 area of 120 km² (Zolotarev and Kharkovets, 2012) (Fig. 1). Mt. Elbrus is an active volcano
159 but only minor fumarole activity is currently observed (Laverov et al., 2005).

160 Elbrus glaciers are situated in the altitudinal range from 2800 m to 5642 m. The
161 stratigraphy records display several ice formation zones on Mt. Elbrus (Bazhev and Bazheva,
162 1964; Psareva, 1964; Troshkina, 1968). The coldest conditions have been observed above
163 5200 m a.s.l., where the mean summer air temperature does not exceed 0 °C. Part of the
164 Elbrus glaciers above 4700–4900 m falls to the zone with limited surface melting. The
165 alternation of the infiltration ice lenses 30 cm thick with the firn horizons was observed in the
166 sequence of snow-firn pack at 5050 m a.s.l. (Mikhalenko, 2008). Two years (1985 and 1988)

167 measurements at the col of Elbrus (5300 m) (Fig. 1c) provided recorded snow accumulation
168 of 400–600 mm w.e. a⁻¹ and considerable wind-driven snow erosion. The snow/firn
169 temperature measured at the col at 6 m depth was -14 °C, indicating absence of melt water
170 runoff from this zone.

171 Long term (since 1983) mass-balance records of the Garabashi glacier show negative
172 values since 1994. In recent years, a negative trend in these values was discovered, which has
173 been accorded by extremely high summer temperatures and glacier melting. The Garabashi
174 glacier elevation has been decreasing at 3.2 m near the equilibrium line for the last decade
175 (Nosenko et al., 2013).

176 A 76 m long ice core was recovered in the accumulation area of the Garabashi Glacier
177 at 3950 m a.s.l. in 1988 (Zagorodnov et al., 1992). The firn completely transforms into ice as
178 a result of melt water refreezing and compression at 23–24 m depth after having been
179 deposited over 7–8 years at negative temperatures. Thus, the geochemical profiles obtained
180 from the ice core were smoothed by melt water percolation and could not be used for
181 paleoclimate and environmental reconstruction.

182 The next ice core was recovered at the Western Plateau of Mt. Elbrus, located at the
183 western slope of Elbrus at 5115 m a.s.l. (Fig. 1). Its area is about 0.5 km². The plateau is
184 restricted on south and south-east by two lava ridges, and by a vertical wall of Mt. Elbrus on
185 the east. During the first probe ice core drilling campaign in 4–6 July 2004 a 21.4 m ice core
186 has been recovered, and borehole temperatures and glacier thickness measurements were
187 conducted on the Western Elbrus Plateau (Mikhalenko et al., 2005). The 10-m depth
188 temperature of -17 °C indicated that any meltwater refreezes at some centimeters below the
189 surface and preservation of isotopic and soluble ions profiles is provided. Ice-core records of
190 this first shallow ice core indicated good preserved seasonal stable isotopic ($\delta^{18}\text{O}$ and δD)
191 oscillations and mean annual accumulation rate was estimated about 1200 mm w.e.

192

193 **2.3 Climatology of the Caucasus and the Mount Elbrus**

194

195 The atmospheric circulation pattern in the Caucasus is determined by the subtropical high
196 pressure in the west and Asian depression in the east dominating in summer time. In winter, it
197 is affected by the western extension of the Siberian high (Volodicheva, 2002). The Caucasus
198 is located in the southern part of the vast Russian Plain permitting unobstructed passage of
199 cold air masses from the north. High elevated ridges on the south prevent and deflect the air
200 flowing from the west and south-west. The influence of the free atmosphere for Elbrus glacier

201 regime is significantly larger than local orographic effects as the glacier accumulation area
202 lies above main ridges.

203 Most of the annual precipitation occurs in the western part of the Caucasus, reaching
204 3240 mm a⁻¹ at Achishkho weather station (1880 m) and in the southern Greater Caucasus.
205 Precipitation ranges between 2000 and 2500 mm a⁻¹ at 2500 m in the west and declines to
206 800–1150 mm a⁻¹ in the east on the northern macroslope of the Caucasus; it ranges eastward
207 from 3000–3200 mm a⁻¹ to 1000 mm a⁻¹ for the southern macroslope. The proportion of
208 winter precipitation (October–April) also declines eastward from more than 50 % to 35–40 %
209 for the northern Greater Caucasus and from 60–70 % to 50–55 % for the southern slope
210 (Rototaeva et al., 2006). The proportion of solid precipitation increases with altitude and
211 reaches 100 % above 4000–4200 m. Following this continental climate effect, the altitude of
212 the glacier equilibrium line (ELA), tends to increase from 2500–2700 m in the Belaya, Laba
213 and Mzymta river basins in the west to 3700–3950 m in the Samur and Kusurchay basins in
214 the eastern sector of the northern macroslope of the Caucasus.

215 Mean summer (May–September) air temperature at ELA ranges from west to east from
216 6–7 °C to 1–2 °C. The ELA is much higher on the glaciers of the northern macroslope, which
217 is distinct in the central Caucasus where ELA on the northern slope of Mt. Elbrus is 1000 m
218 higher than on Svanetia glaciers 80 km southward. The number of high-elevated
219 meteorological stations is very limited in the Caucasus. Figure 2 shows the mean monthly air
220 temperature and precipitation at the Klukhor Pass, Teberda and Terskol meteorological
221 stations in the western and central Caucasus (Figure 1 and Table 1).

222

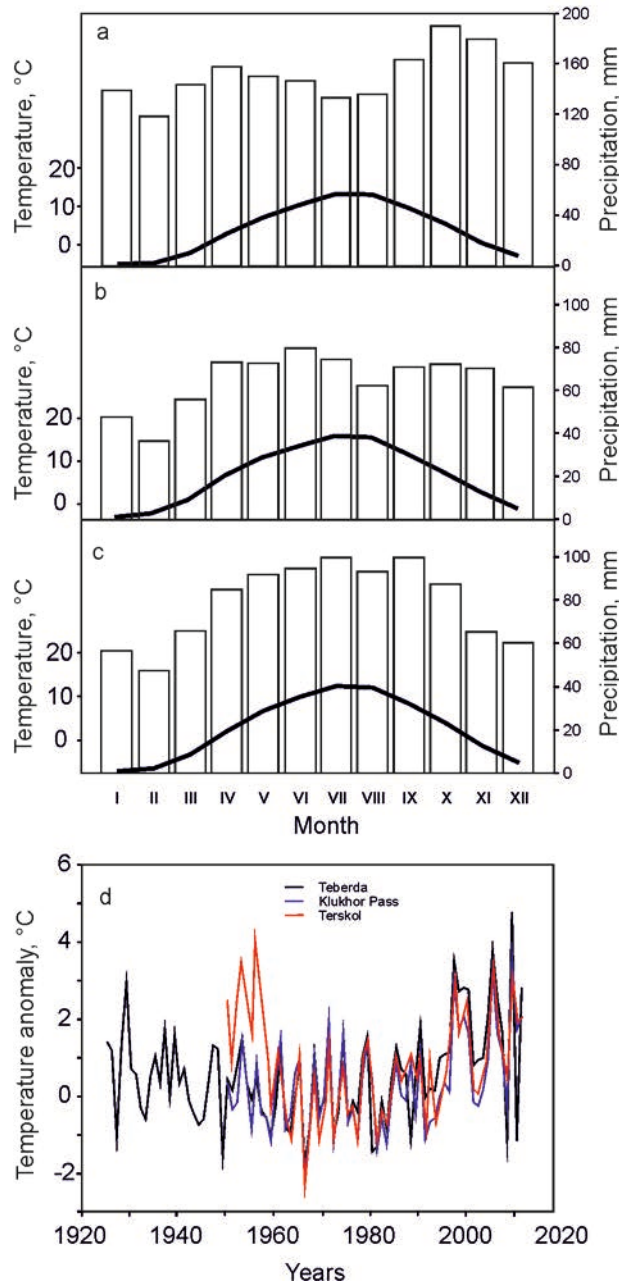
223 Table 1. Meteorological data used in this work (modified from Solomina et al., 2012)

Meteorological station	Geographical coordinates	Altitude, m	Beginning of observation
Klukhor Pass	N 43°15'; E 41°50'	2047	1956
Teberda	N 43°27'; E 41°44'	1313	1956
Terskol	N 43°15'; E 42°30'	2214	1951
Mineralnie Vody	N 44°14'; E 43°04'	316	1955

224

225 Air temperatures at these stations are in good agreement and correlate well with lowland
226 stations ($r = 0.7–0.9$, $p < 0.01$), and this indicates the homogeneity of the temperature regime
227 for investigated area (Solomina et al., 2012). Variation of mean annual and monthly
228 temperature for the Klukhor Pass station for the period of observation (see Table 1) does not
229 display statistically significant trend. A positive trend for mean annual temperature ($r = 0.33$,
230 $p < 0.05$) and slight positive trend for summer temperature was found for the Teberda station.
231 Temperature records from the Terskol station located 7 km southward apart from Elbrus

232 glaciers show a negative mean annual temperature trend for the whole period of observation
 233 ($r = -0.35, p < 0.05$) (Solomina et al., 2012) but mean summer (May–September)
 234 temperatures increased from 11.5 °C in 1987–2001 period to 12.0 °C over the last decade.
 235 Winter precipitation increased by 20% over the same period while summer precipitation did
 236 not show any change (Nosenko et al., 2013).



237
 238 Figure 2. Mean monthly air temperature and precipitation at the Klukhor Pass (a), Teberda
 239 (b), and Terskol (c) meteorological stations and (d) anomalies of mean summer temperature,
 240 deviations from the average 1961–1990 value.

241

242 First meteorological measurements were taken on the Elbrus glaciers in 1934–1935 by
 243 the expedition of the Academy of Sciences of the USSR (Baranov and Pokrovskaya, 1936).

244 Air temperatures, pressure, humidity, wind regime, and incoming solar radiation have been
245 measured at four sites from Terskol at 2214 m to the col of Elbrus at 5300 m. A permanent
246 meteorological station was established near Priyut-9 on the southern slope of the Garabashi
247 Glacier at 4200 m in 1934. According to 1949–1952 data, mean annual air temperature of
248 $-9.2\text{ }^{\circ}\text{C}$ was observed. The temperature of the coldest month (January) was $-17.1\text{ }^{\circ}\text{C}$, July
249 temperature was $-0.5\text{ }^{\circ}\text{C}$. The minimum air temperature of $-36.1\text{ }^{\circ}\text{C}$ was measured on
250 January 30, 1950, with a maximum of $10.7\text{ }^{\circ}\text{C}$ on August 1, 1950. Annual precipitation rate of
251 1128 mm was observed for 1949–1952. The summer months (April–October) contribute 75 %
252 of the total precipitation, while the winter months (November–March) account for only 25 %
253 (Matyuhkin, 1960). Maximum wind speed at Priyut-11 station of 56 m s^{-1} was measured in
254 January 1952.

255 During the IGY (1957–1959) the permanent all-year meteorological station was
256 established on the Glacier Base on the southern slope of the Elbrus near glaciers at 3700 m.
257 Meteorological records from this site include diurnal air pressure and temperature,
258 precipitation, humidity, cloudiness, wind regime and snow cover thickness (Tushinskii, 1968).
259 Heat balance, air temperatures, wind speed were recorded during occasional observations in
260 the col of Mt. Elbrus (5300 m). First accumulation and ablation measurements on the southern
261 slope of Mt. Elbrus were done during the IGY and in 1961–1962 (Bazhev and Bazheva, 1964).

262

263 **3 The Western Elbrus Plateau glacier archive**

264

265 In the following section we will present recent meteorological, glaciological and glacio
266 chemical investigations conducted on the Western Elbrus glacier plateau with the aim of
267 obtaining knowledge about the suitability of this site to obtain atmospheric relevant ice core
268 records.

269

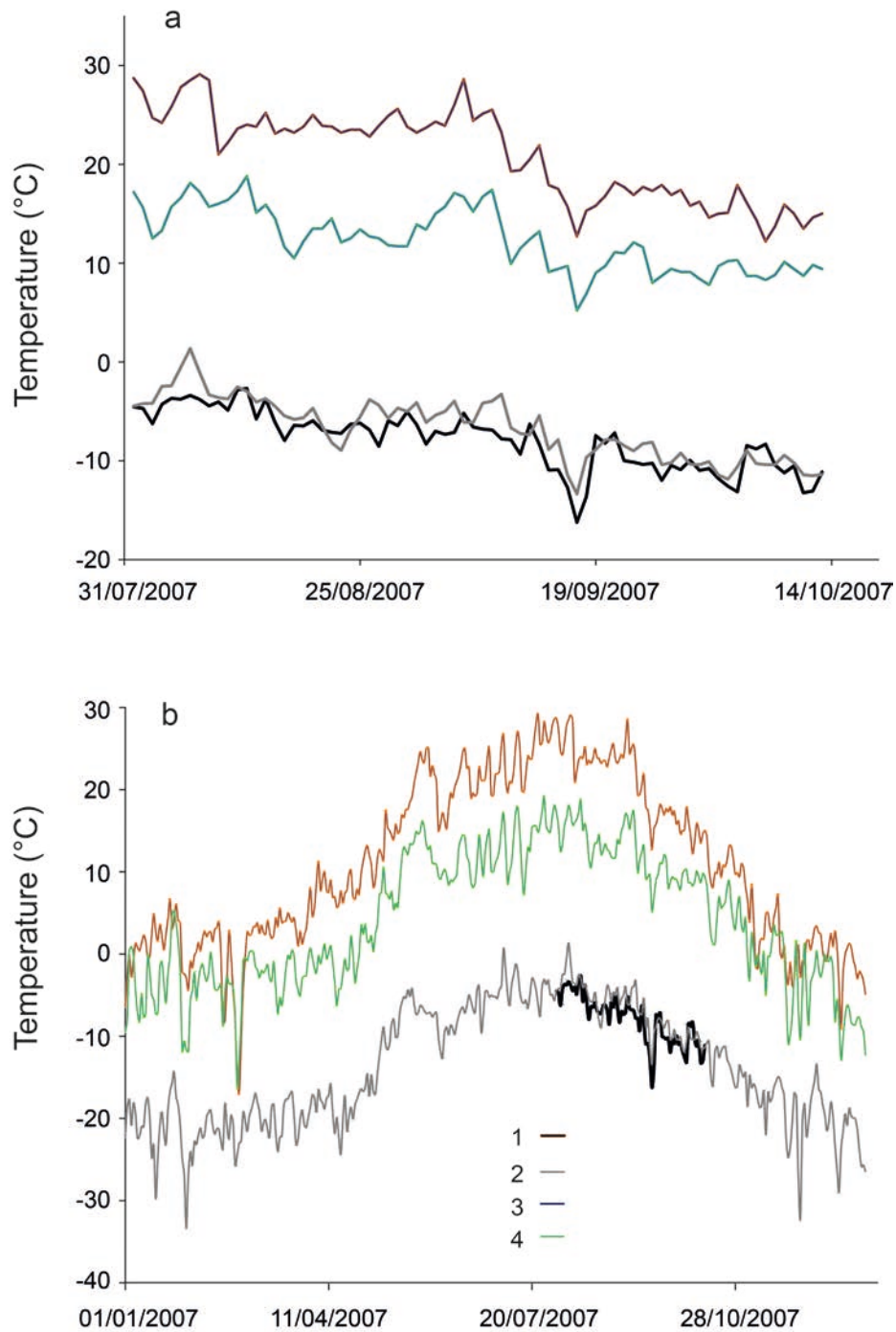
270 **3.1 On site meteorological measurements**

271

272 An automatic weather station (AWS) of AANDERAA Data Instruments was installed on the
273 Western Elbrus Plateau at 5115 m a.s.l. at the drill site in 2007. The AWS was working
274 between July 30, 2007, and January 11, 2008, but disappeared afterwards under unascertained
275 circumstances. Here we discuss records until the October 12, 2007, only when consistent data
276 without voids was obtained. Air temperature, wind speed and direction, humidity, air
277 pressure, radiation balance, and snow cover thickness have been measured with the time
278 resolution of 1 hour. According to AWS records, mean daily air temperatures were negative

279 during the period of observations. One hour averaged temperature also was negative while the
280 positive instant maximum air temperature was recorded on eight occasions and ranged from
281 0.1 °C to 3.1 °C. Average wind speed (one hour averaged) on the drilling site of 2.9 m sec⁻¹
282 was measured over the whole period of observation. Wind gusting up to 21.4 m sec⁻¹ was
283 observed in frontal passage and cyclone rear, while mean daily maximal wind speed was 6.7
284 m sec⁻¹ in August–September 2007. Our data did not cover the whole year but according to
285 measurements of 1961–1962 the average wind speed was approximately 30% higher in
286 Winter at the southern slope of Elbrus (Tushinskii, 1968). A combination of high snow
287 accumulation and low average wind speed with prevailing westerlies allows us to assume that
288 most of precipitation was deposited at the disposal site and was not scoured by wind.

289 AWS records were compared with the records of the measurements at the mountain
290 meteorological station Kluhor Pass (2037 m a.s.l.; 50 km westward) and lowland Mineralnie
291 Vody station (316 m a.s.l.; 120 km north–eastward) (Table 1) as well as with the 20th century
292 Reanalysis V2 data provided by the NOAA/OAR/ESRL PSD, Boulder, Colorado, USA,
293 (<http://www.esrl.noaa.gov/psd/>) (Fig. 3 a, b). Temperature lapse rate of 0.6° per hundred m
294 elevation was observed during the summer months. In winter, however, it decreases due to
295 temperature inversions at the Mineralnie Vody station. There is a good agreement between the
296 temporal variation of mean daily air temperature measured by the AWS at the drill site, 20th
297 Century Reanalysis and meteorological stations data ($r > 0.85$). Therefore the temperature
298 variations at the West Elbrus plateau follow the regional temperature regime.



299
 300 Figure 3. Daily temperature averages (T , °C) for the period of 1 August–12 October 2007 (a)
 301 and 1 January–31 December 2007 (b): 1 – AWS at the Western Elbrus Plateau; 2 – 20th
 302 Century Reanalysis V2; 3 – Mineralnie Vody meteorological station; 4 – Klukhor pass
 303 station.

304
 305 In June 2013, main meteorological observations with AWS DAVIS Vantage Pro 2
 306 including air temperature, humidity and wind speed at two levels (0.5 and 2.0 m) with 15 min
 307 resolution were conducted at the Western Elbrus Plateau near the drilling site of 2009 (see
 308 Figure 1 and 4). Along with the estimation of eddy flux of heat and moisture, the fluxes of

309 total, scattered and reflected radiation were measured. Meteorological conditions of the
310 observation period with maximum insolation at the summer solstice were close to mean
311 annual parameters. A level of downward shortwave radiation was varied from 1 to 1.2 kW
312 m⁻² adding up to 73–88 % from solar constant at the outer boundary of the atmosphere and
313 78–93 % of total insolation at N 43° latitude at that time of year. Albedo has a dominant role
314 in the short wave balance. Mean albedo values of 0.66 were measured at the plateau in June
315 2013. First measurements of radiation balance were conducted in Elbrus in 1968–1960 and
316 showed that downward short wave radiation ranged from 1.1 kW m⁻² at an elevation of 3750
317 m up to 1.2 kW m⁻² at 5300 m (Tushinskii, 1968).

318 Despite the negative air temperatures, the radiation balance was positive except at night
319 time. The mean value of the radiation balance, including short-wave and long-wave balance
320 of 150 W m⁻² was measured. Apparently, this is just the power that was expended for surface
321 melting and snow recrystallization.

322

323 **3.2 Ground base survey: surface topography and radar sounding**

324

325 Detailed measurements of ice thickness were carried out in 2005 and 2007 using monopulse
326 ice penetrating radar VIRL with the central frequency of 20 MHz (Vasilenko et al., 2002,
327 2003). VIRL ice penetrating radar consists of transmitter, receiver and digital recording
328 system with GPS. For synchronization of transmitter and receiver a special radio channel with
329 repetition rate of 20 MHz was used in 2005. Advanced VIRL–6 radar modification with
330 optical channel for synchronization has been used in 2007 (Berikashvili et al., 2006). The
331 radar allows simultaneous recording and controlling in a real time regime with an interval
332 from 1 to 99 sec to get both radar and navigation data as well as to perform the hardware and
333 program stacking (from 1 to 6192-times) of wave traces.

334 The average radio wave velocity (RWV) in firn and ice has been used for ice thickness
335 calculation from measured time delay of radar signals reflected from the bedrock. RWV
336 depends on firn/ice density and temperature. We did not measure RWV (V) at the Western
337 Elbrus Plateau, but it has been estimated as a function of glacier depth (z) through measured
338 ice core density $\rho_d(z)$ and borehole temperature T (z) profiles:

339

$$340 \quad V(z) = c/[\epsilon'(\rho_d, T)]^{1/2}, \quad (1)$$

341

342 where $c = 300 \text{ m } \mu\text{s}^{-1}$ – radio wave velocity in air; $\epsilon'(\rho_d, T)$ – dielectric permeability of snow, firn
343 and ice as a function of density $\rho_d(z)$ and temperature T(z) (Macheret, 2006).

344 $\epsilon'(\rho_d)$ was calculated for two component dielectric mixture of ice and air (Looyenga, 1965):

345

346
$$\epsilon'(\rho_d, T) = \{(\rho_d/\rho_i)[\epsilon'_i(T)^{1/3} - 1] + 1\}^{1/3}, \quad (2)$$

347

348 where $\rho_i = 917 \text{ kg m}^{-3}$ – density of glacier ice.

349 $\epsilon'_i(T)$ was calculated from (Mätzler and Wegmüller, 1987):

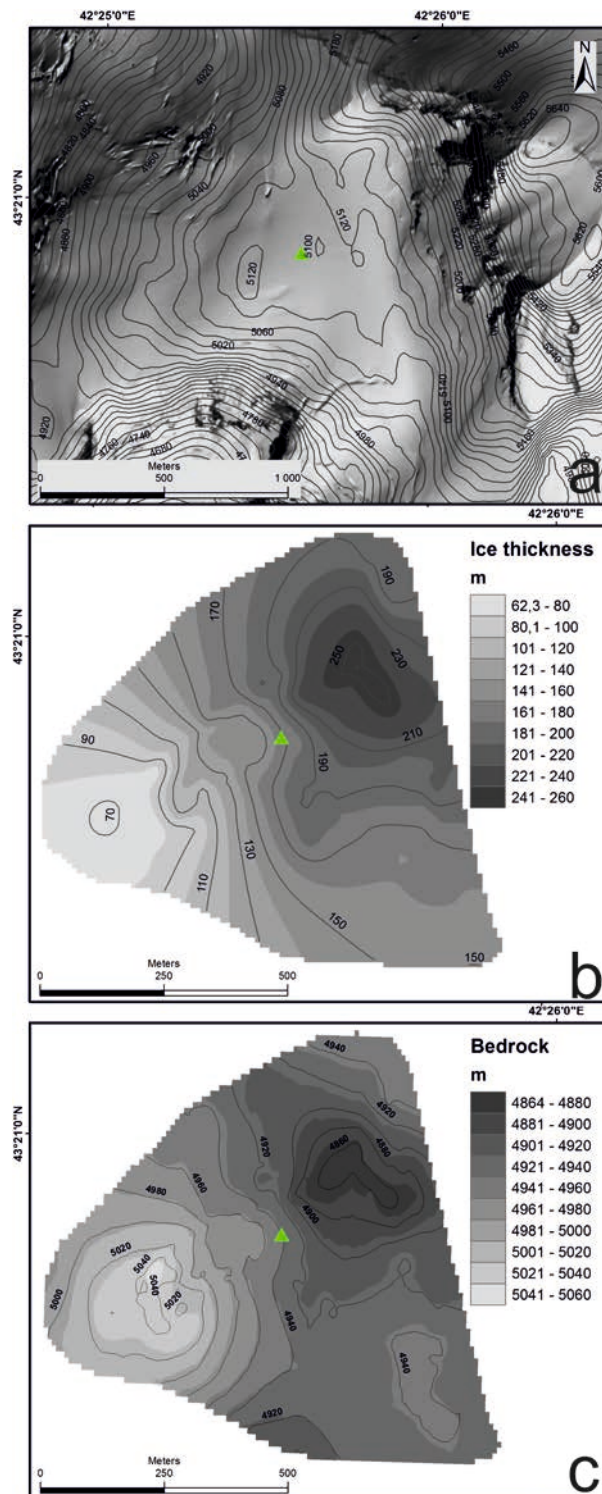
350

351
$$\epsilon'_i(T) = 3.1884 + 0.0091 T. \quad (3)$$

352

353 The average RWV of $180 \text{ m } \mu\text{s}^{-1}$ was calculated for 181.8 m (ice thickness at the
354 drilling site). RWV taking into account its depth variations from ρ_d and T has been used for
355 conversion of the measured time delay of radio signal to ice thickness at each point.

356 Two data sets, 2005 and 2007, have been combined to construct an ice thickness map.
357 In total, the glacier depth was measured at more than 10000 sounding points along 6.5 km
358 profiles with the estimated accuracy of ice thickness measurements of 3% (Lavrentiev et al.,
359 2010). The maximum depth of 255 ± 8 m at the central part of the plateau, minimum values of
360 about 60 m near the edge were found. Radar records and digital elevation model ASTER
361 GDEM averaged for 2000–2009 have been used for bedrock topography mapping (Fig. 4).
362 ASTER GDEM with an error of ± 20 m (ASTER..., 2009) is in a good agreement with the
363 1959 Northern Caucasus topographic map and the 1997 digital orthophotomap of Mt. Elbrus
364 (Zolotarev and Kharkovets, 2000).



365

366 Figure 4. Glacier surface (a), ice thickness (b), and bedrock relief (c) on the Western Elbrus
 367 Plateau. The green triangle marks the position of the drilling site.

368

369 3.3 Ice core drilling and analysis

370 3.3.1 Methods

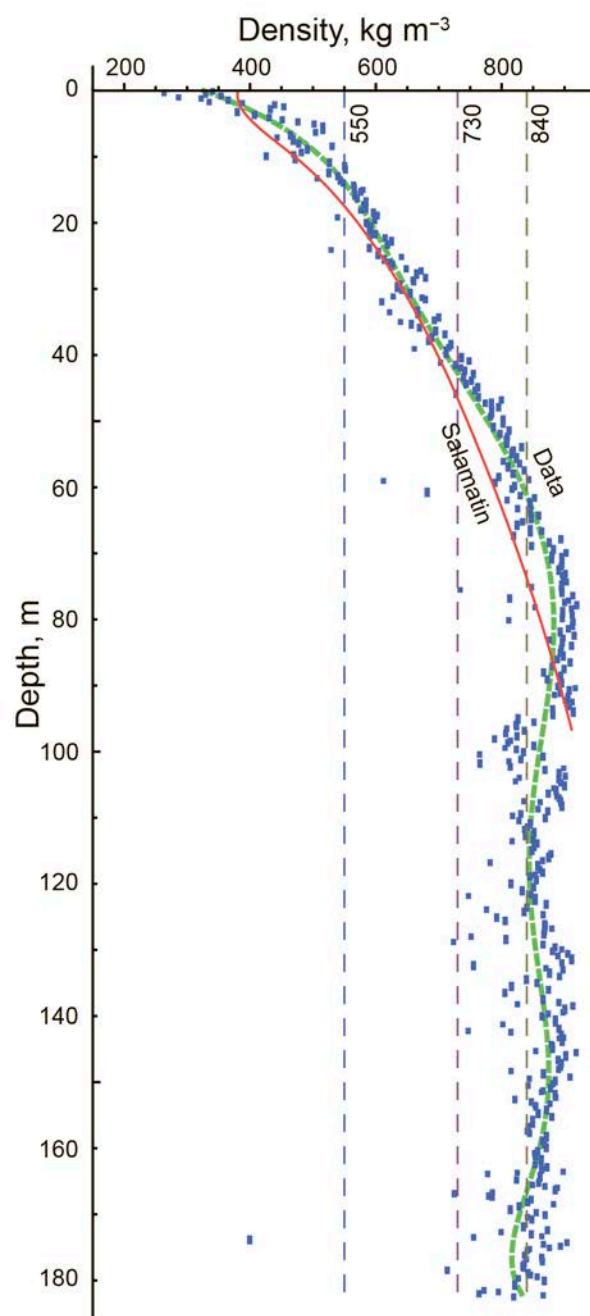
371

372 Due to the promising glacier archive conditions obtained from the shallow ice coring in 2004
 373 (see section 2.2), a full-depth ice core drilling was completed on the Western Plateau from 27

374 August to 6 September 2009 (Mikhalenko, 2010). A bedrock was reached at the depth of
375 181.80 m. Drilling was done in a dry borehole using the lightweight electromechanical
376 drilling system developed by Geotech Co. Ltd., Nagoya, Japan. Technical details of the drill
377 are described in (Takeuchi et al., 2004). The recovered ice cores were subjected to
378 stratigraphic observations, packed into plastic sleeve and stored in the snow pit under $-10\text{ }^{\circ}\text{C}$.
379 Ice core drilling was accompanied by borehole temperature measurements (using thermistor
380 chains which were left for three days in the borehole and calibrated before and after study
381 with an error of $\pm 0.1\text{ }^{\circ}\text{C}$), and snow pit sampling 30 m to the south from the drilling site. The
382 ice core was shipped in frozen condition to the cold laboratory of the Lomonosov Moscow
383 State University where detailed stratigraphic descriptions with photographing of each piece of
384 the core and bulk density measurements were done.

385 In addition to the 2009 ice core subsequent ice core (12 m long) was extracted in June
386 2012 at the same site to expand the existing ice core sample set from this site to the year 2012.
387 Note that, among others the 2012 ice core was also used for the dust study of Kutuzov et al.
388 (2013). Finally, in June 2013, a 20.36 m depth was recovered at the same location from 27 to
389 30 June 2013.

390 Stratigraphic description of the ice core was carried out using transmitted-light
391 illumination. Hereby, stratification depth and thickness of individual horizons were fixed with
392 1 mm accuracy. Density of firn and ice were measured by 457 individual samples. Figure 5
393 shows the bulk density distribution with depth. The sharp random outliers from the general
394 profile in both directions, but more often to lower values, could result from uncertainties in
395 estimation of lengths of samples. The uncertainty increases for the denser and smaller
396 samples.



397

398 Figure 5. Measured (blue dots) and simulated (red line) ice core density profile, critical
 399 densities shown as dashed lines (see 3.3.2.). The green dashed line is a running mean for the
 400 measured density values.

401

402 Ionic species as ammonium (NH_4^+) succinate ($\text{HOOCCH}_2\text{COO}^-$, also denoted succinic
 403 acid) were investigated along the uppermost 157 m of the Elbrus core (122 m w.e.) with the
 404 aim of the ice core dating. Hereby, the analytical protocol previously developed to process
 405 Alpine firn and ice samples (Legrand et al., 2007a) was applied. Pieces of firn and ice were
 406 decontaminated in a clean air bench located in a cold room using a pre-cleaned electric plane
 407 tool. A total of 3350 subsamples were obtained along the 157 m with a depth resolution
 408 decreasing from 10 cm at the top to 2 cm at 157 m depth.

409 For cations (Na^+ , K^+ , Mg^{2+} , Ca^{2+} , and NH_4^+), a Dionex ICS 1000 chromatograph
410 equipped with a CS12 separator column was deployed. For anions, a Dionex 600 equipped
411 with an AS11 separator column was used with an eluent mixture made on the base of H_2O ,
412 NaOH at 2.5 and 100 mM and CH_3OH . A gradient pump system allows determining
413 inorganic species (F^- , Cl^- , NO_3^- , and SO_4^{2-}) as well as short-chain monocarboxylates
414 (denoted MonoAc^-) and dicarboxylates (denoted DiAc^{2-}). For all investigated species, ion
415 chromatography and ice core decontamination blanks were found to be insignificant with
416 respect to respective levels found in the ice core samples.

417 As discussed in Sect. 3.3.5 the search of volcanic horizons in the Elbrus ice cores needs
418 examination of the acidity (or alkalinity) of samples that can be evaluated by checking the
419 ionic balance between anions and cations (concentrations being expressed in micro-
420 equivalents per liter, $\mu\text{Eq L}^{-1}$):

421

$$422 \quad [\text{H}^+] = ([\text{F}^-] + [\text{Cl}^-] + [\text{NO}_3^-] + [\text{SO}_4^{2-}] + [\text{MonoAc}^-] + [\text{DiAc}^{2-}]) - ([\text{Na}^+] + [\text{K}^+] + [\text{Mg}^{2+}] + \\ 423 \quad [\text{Ca}^{2+}] + [\text{NH}_4^+]). \quad (4)$$

424 Within the present study, we focus (see also section 3.3.4) on the NH_4^+ and succinic
425 acid profiles, in view to (1) define a criterion which allows to separate winter and summer
426 snow depositions, (2) to apply this criterion on the first 157 m of the Elbrus ice core to the
427 establish a depth age relation on the basis of annual layer counting along the NH_4^+ and
428 succinic acid depth profile.

429 The 2012, 2013 as well as the 2009 ice core (down to 106.7 m) were analyzed for
430 deuterium-hydrogen (D/H) and oxygen ($^{18}\text{O}/^{16}\text{O}$) isotope ratios using Picarro L1102-*i* instrument
431 in the Climate and Environmental Research Laboratory (CERL), Arctic and Antarctic Research
432 Institute, St. Petersburg, Russia. The instrument was calibrated on a regular basis against isotopic
433 standards V-SMOW, GISP and SLAP provided by the International Atomic Energy Agency
434 (IAEA) for estimating the precision of the measurements and for minimizing the memory effect
435 associated with continuous measurements. The reproducibility of the measurements was ± 0.07
436 ‰ for oxygen isotope ($\delta^{18}\text{O}$) and ± 0.3 ‰ for deuterium (δD). The CERL laboratory work
437 standard SPB was measured after every 5 samples. The $\delta^{18}\text{O}$ and δD values were expressed in ‰
438 units relative to the V-SMOW value.

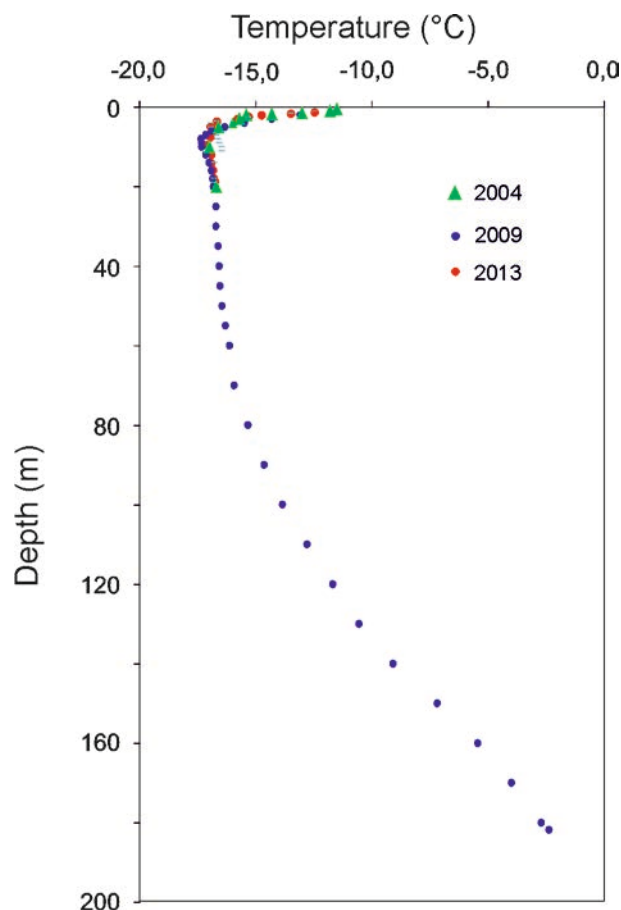
439

440 **3.3.2 Borehole temperatures**

441

442 Figure 6 shows the vertical profile of the temperature measured along the 181 m long
443 borehole drilled in 2009. Temperatures ranged from -17 °C at 10 meters depth to -2.4 °C at

444 181.8 m. The temperature profile can be divided into three parts on the base of different
 445 gradient of temperature: from the surface down to 10 m, from 10 m to 100 m, and from 100 m
 446 to glacier bottom. Upper part of the temperature profile reflects seasonal changes at the
 447 surface. The borehole temperature ranges from $-17\text{ }^{\circ}\text{C}$ to $-12\text{ }^{\circ}\text{C}$ within 10–100 m, and most
 448 accurately reflects the past temperature fluctuations. Temperature change is almost rectilinear
 449 from 100 m depth to glacier bottom that gives evidence of a steady heat transfer regime.
 450 Density of heat flux at the glacier bottom of 0.34 W m^{-2} was calculated from measured
 451 temperature gradient and the coefficient of heat conductivity of ice (2.25 W m^{-2}). This value
 452 is 4–5 times higher than averaged heat flux density for the Earth surface and higher than the
 453 mean value for Central Caucasus, and associated with heat magma chamber of the Elbrus
 454 volcano. Fig. 6 also shows the temperature profile measured in the 19-m depth borehole in
 455 2013 and temperature records obtained in 2004 after 22-m depth shallow ice core drilling on
 456 the Plateau (Mikhalenko et al., 2005). Good record matching is indicative to stable
 457 temperature regime on the Western Elbrus Plateau for the last decade.



458
 459 Figure 6. Measured temperature profiles at the Western Elbrus Plateau drill site for different
 460 dates: and green triangles – 22 m depth borehole drilled in 2004, blue dots – main 2009
 461 borehole, and red dots – 20 m depth borehole drilled in 2013.

462

463 Using the altitude gradient of temperature estimated in section 3.1 on the base of
464 temperature data obtained from the AWS station run at the Western Elbrus Plateau not far
465 from the 2009 drill site and the low elevation station Mineralnie Vody, we estimate the annual
466 mean air temperature at the drill site to be around -19°C . This is close to value of annual
467 mean air temperature of -19.4°C which was calculated using the general relationship with
468 the ice temperature at the bottom of the active layer (Zagorodnov et al., 2006) and only
469 slightly enhanced compared to the 10 m firn temperatures (see above).

470 The analysis of measured temperature profile shows that bottom melting can occur
471 under real ice pressure at the deepest part of the glacier. Potential bottom melting has been
472 estimated using mathematical model of temperature regime (Salamatin et al., 2001). Modeling
473 results show that bottom melting occurs under ice thickness more than 220 m and its value
474 does not exceed 10 mm w.e. y^{-1} .

475

476 **3.3.3 Bulk density and ice core stratigraphy**

477

478 The bulk density profile suggests a change in densification around the critical densities
479 (Maeno and Ebinuma, 1983) of 550 and 840 kg m^{-3} , and no visible change at 730 kg m^{-3} , which
480 is also the case in some other analyses of density profiles (Hörhold et al., 2011; Ligtenberg et al.,
481 2011). However, the slight trend of a decrease in density at a depth below the maximal values at
482 about 80 m (Fig. 5), close to the critical density over the whole depth interval, is unlikely to be a
483 systematic error in measurements and need further investigation. The research should be based
484 on the ice flow characterization and the possible effects related to the “intervening depth
485 interval” (the alternating of the layers, which have already reached the close-off density, with
486 those which are still permeable) due to seasonal (Bender et al., 1997) or wind induced (seasonal
487 difference in wind speed) snow density variability at high accumulation sites, which are
488 accounted for. Unlike the ice cores from polar ice sheets where such “intervening depth interval”
489 is just a fraction of the whole length of the ice core (Bender et al., 1997), the measured bulk
490 density in the Elbrus ice core remains at a wide interval between 800 kg m^{-3} and 915 kg m^{-3}
491 down to the bottom of the glacier (Figure 5). Elbrus’s profile was compared with the results of
492 the Salamatin et al. (2009) densification model. Modelling results show that there has been an
493 increase in the accumulation rate over the past several years. Minimum deviation between
494 simulated and measured ice-core density profiles was marked when the accumulation history
495 was assumed in accordance with the long-term precipitation changes observed at meteorological
496 stations (Nosenko et al., 2013).

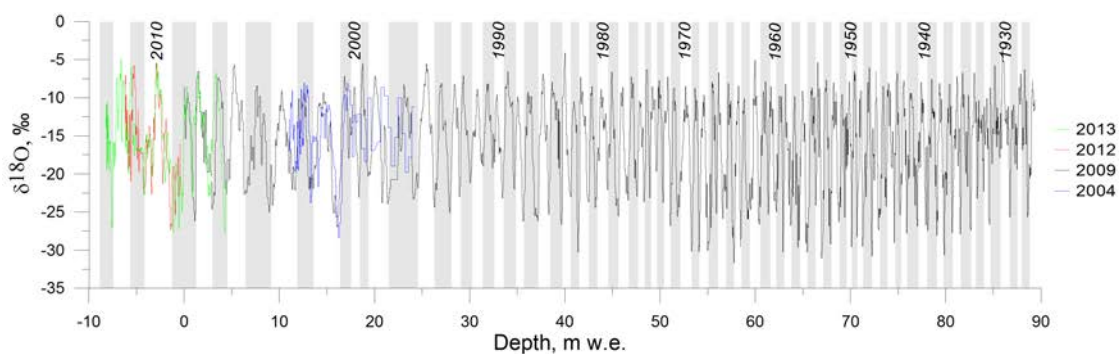
497 According to the morphogenetic classification of stratigraphic features (Arkhipov et al.,
 498 2001) two distinct types of layering were observed in the core: firm layers which have not
 499 been affected by melting, and ice layers formed by the refreezing of melt water in the surface
 500 snow. These features indicate that the thickness of the infiltration ice layers, which do not
 501 form every year, does not exceed 10 mm. Ice formation occurs in cold, dry conditions, as
 502 already concluded on the basis of borehole and air temperatures at the drill site (see sections
 503 3.1 and 3.3.2). The pore close-off depth at around 55 m, where the air bubbles became
 504 separated, was marked. This depth coincides with a measured bulk density of around 840 kg
 505 m⁻³. This is no surprise, since the presence of ice layers will increase the close-off density
 506 somewhat above the density close-off value from ice in which no melting occurs (i.e. 830 kg
 507 m⁻³).

508

509 3.3.4 Seasonal ice core stratigraphy of stable water isotopes

510

511 Seasonal cycle of the isotopic composition is well detectable over the whole measured part of the
 512 core (Fig. 7). Mean seasonal values of δD are -200‰ for the winter period and -25‰ for the
 513 summer period. Values of $\delta^{18}O$ are about -5 to -10‰ in summer and -30‰ in winter.
 514 According to isotopes annual cycles counting 106.7 m of the ice core cover 86 years or the
 515 period from 1924 to 2009. Mean accumulation rate for this period based on the dating and taking
 516 into account the firm density and layer thinning was 1455 mm w.e. Figure 7 shows results of
 517 isotopic measurements of four different ice cores obtained at the Western Elbrus plateau. While
 518 2009, 2012 and 2013 cores were obtained almost at the same location the 2004 core was
 519 recovered further 120 m to the south-west. Good agreement in isotopic variations of all cores
 520 suggests a relatively homogeneous snow deposition at the plateau.



521

522 Figure 7. $\delta^{18}O$ profiles in the cores obtained in 2004, 2009, 2012, 2013. 0 m depth
 523 corresponds to the surface of 2009. Grey and white boxes depict annual layers.

524

525 We used the isotope diffusion model (Johnsen et al., 2000) to estimate the preservation of
 526 the isotopic signal in the course of the diffusive smoothing. Although the drilling site is located

527 in a relatively warm place ($-17\text{ }^{\circ}\text{C}$), high snow accumulation rate does not favour a strong
528 diffusion, since any firn layer rapidly sinks and reaches the pore close-off depth in a relatively
529 short time. The maximum “diffusion length” at this depth is estimated as 5 cm in ice equivalent
530 (i.e.). The effective diffusion length could be even smaller if we take into account ice lenses in
531 the firn that prevent vertical travelling of the water molecules.

532 Such a diffusion length means that all the oscillations shorter than 13 cm i.e. will be
533 completely erased due to the diffusion, the oscillations between 13 and 70 cm i.e. will survive
534 but will be damped to some extent, and the cycles longer than 70 cm (e.g., the annual cycle) i.e.
535 will not be affected by the diffusion. Thus, if during a single snowfall a 35-cm snow layer
536 precipitates (that corresponds to 13 cm in i.e.), the isotopic signal of this layer will survive
537 during the diffusion processes and will be seen in the ice core.

538 Deeper than the pore close-off depth the diffusion takes place in ice but much slower than
539 the in firn. The final diffusion length solely depends on the time and temperature of the firn-ice
540 thickness. Even if we take a maximum possible temperature ($-2.4\text{ }^{\circ}\text{C}$) and age estimate (few
541 hundred years), the additional diffusion in ice will still be very small.

542 This leads us to an important conclusion: we may expect to obtain the seasonal cycles in
543 the isotope profile down to the very bottom of the core, and our ability to detect the annual cycle
544 in the core will be dependent on the sampling resolution, as well as on such basal processes as
545 layers folding and mixing.

546

547 **3.3.5 Seasonal ice core stratigraphy of chemical parameters and ice core dating on the** 548 **base of annual layer counting**

549

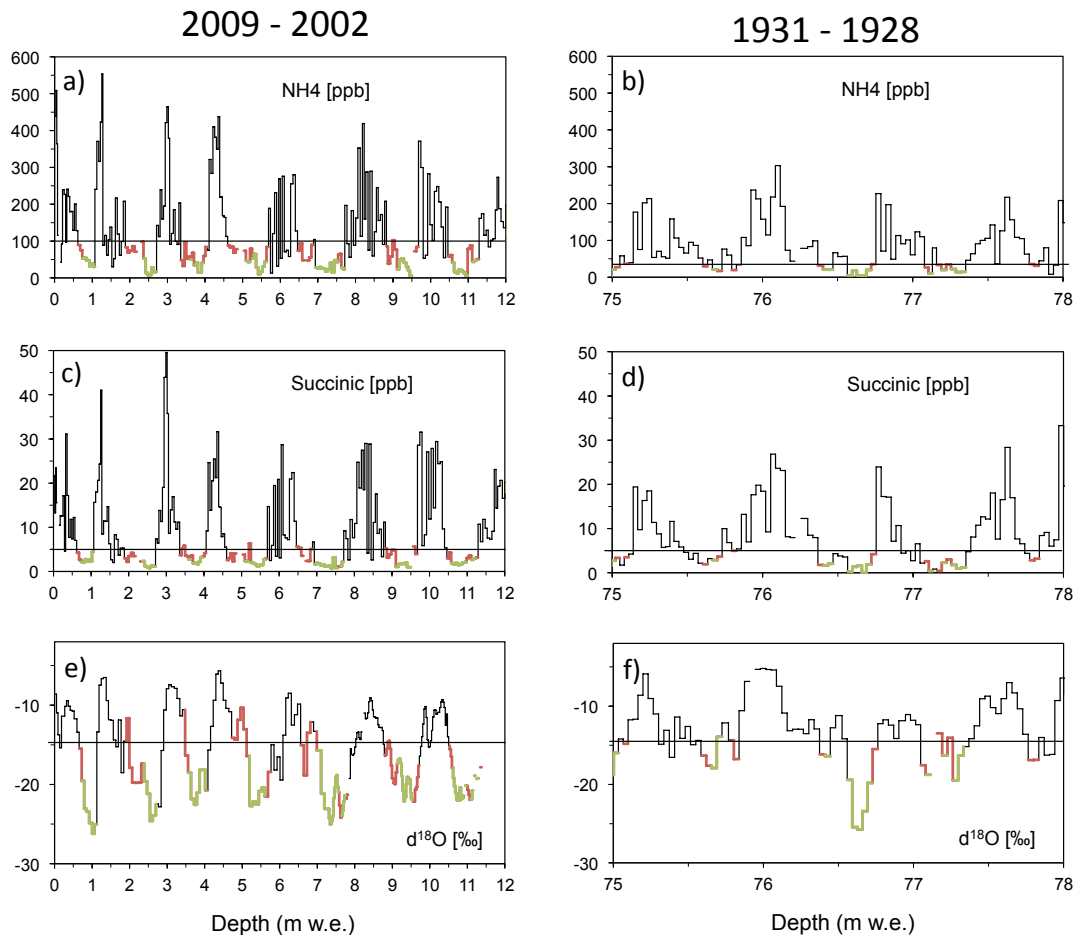
550 A dating attempt was made by counting annual layers on the basis of chemical ice core
551 stratigraphical records, as previously successfully applied to mid-latitude Alpine ice cores
552 (Preunkert et al., 2000). As done in Alpine ice core studies, we examine the NH_4^+ signal.
553 Since this specie experiences a strong maximum of emissions in phase with the summer
554 strengthened of upward transport of air masses, a particularly well-pronounced seasonal cycle
555 is expected, as observed at the Col du Dôme Alpine site (Preunkert et al., 2000; Fagerli et al.,
556 2007). However, it appears that the NH_4^+ seasonal cycle at Elbrus is less pronounced than in
557 the Alps. Whereas recent summer NH_4^+ levels are comparable at both sites, recent winter
558 concentrations at Elbrus are significantly higher than at Col du Dôme.

559 A first study on the seasonality of the Elbrus snow accumulation was made by Kutuzov
560 et al. (2013) along a short firn core spanning the years 2012–2009. Based on the dust layer
561 stratigraphy of absolute dated dust events and the stable isotope record of the firn core the

562 authors showed that the annual deposition at Elbrus has a mean $\delta^{18}\text{O}$ signature of -15‰ and
563 is built up by nearly equal deposition amounts from the warm season (45 % of total
564 accumulation), for which $\delta^{18}\text{O}$ values varying between -5.5‰ and -10‰ , and from the cold
565 season (55 % of total accumulation), for which values vary between -17‰ and -27‰ ,
566 respectively.

567 Therefore, the concentration distribution of NH_4^+ values was inspected in recent firn
568 layers (0–12 m w.e.), and the 50 % concentration limit of 100 ppb was taken as a first
569 approach to separate snow depositions arriving from summer and winter precipitation at
570 Elbrus. However this criterion will be not conservative in time since the NH_4^+ sources are
571 mainly anthropogenic in origin, and a trend in summer as well as in winter are expected over
572 the last 100 years. Therefore, a second criterion was used to confirm our winter snow
573 selection. This criterion used succinic acid, a light dicarboxylic acid for which a strong
574 summer maximum and a quasi-nul winter level can be observed in the present-day
575 atmosphere in Europe (Legrand et al., 2007b), the very low winter levels being related to the
576 absence of source at that season for this species mainly photochemically produced from
577 biogenic precursors. The concentration distribution of succinate values was inspected in
578 recent firn layers (0–12 m w.e.), and the 50 % concentration limit of 5 ppb was taken to
579 separate snow depositions arriving from summer and winter precipitation at Elbrus. Winter
580 snow and ice layers were identified when both ammonium and succinate criteria were fulfilled
581 for more than 2 successive samples.

582 Figure 8 a, c shows the result of this data dissection over the uppermost 12 m w.e. along
583 with the $\delta^{18}\text{O}$ record (Fig. 8 e). The mean $\delta^{18}\text{O}$ level of hereby selected winter data is -19.6
584 ‰ , and as it could be detected in Fig. 8 a, c from ammonium and succinate selected winter
585 sections match quite well with winter sections deduced from the $\delta^{18}\text{O}$ profile. However it
586 might appear that sometimes the spring season or even the beginning of the summer season
587 might be included. For an application as the dating by annual layer counting this shortcoming
588 is not critical, however if an inspection of the data set in seasonal resolution is envisaged this
589 might be a handicap. In this case a stronger criteria ($\text{NH}_4^+ < 50$ ppb and succinate < 3 ppb)
590 might be applied in addition to assure that only depositions corresponding to winter
591 precipitation under atmospheric background conditions are selected within the winter period.
592 The mean $\delta^{18}\text{O}$ level of hereby selected winter data is -21.1‰ . On the other hand, as seen in
593 Figure 8 a, c, and e some winter sections might be omitted.



594

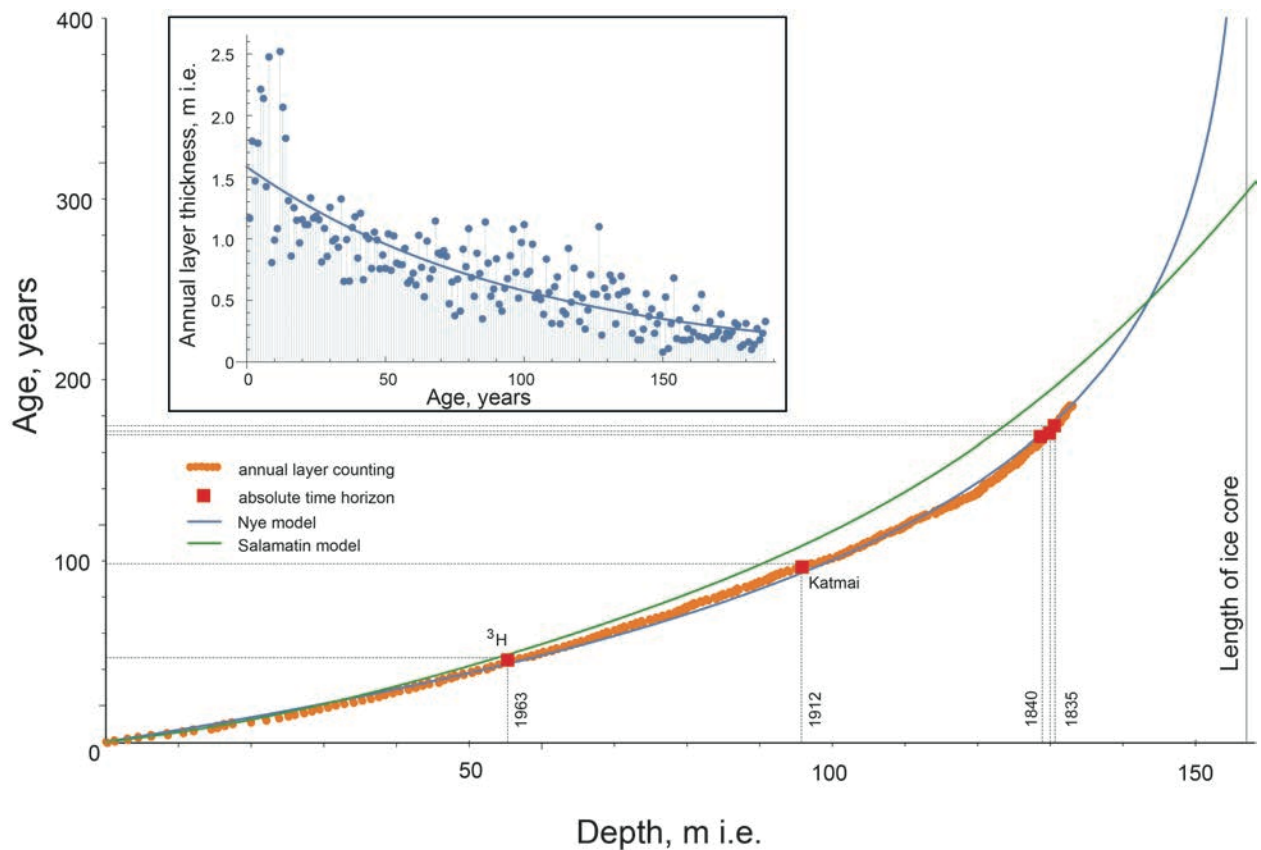
595 Figure 8. Seasonal course of NH_4^+ (a, b), succinic acid (c, d), and $\delta^{18}\text{O}$ (e, f) signals at to
 596 different sections of the Elbrus ice core. Red marked sections assigned samples selected with the
 597 winter criterion: Succinic acid smaller than 5 ppb, NH_4^+ smaller than 100 ppb for recent years
 598 and smaller than 50 ppb prior to 1950; green marked sections correspond to the winter-
 599 background criterion: Succinic acid smaller than 3 ppb, NH_4^+ smaller than 50 ppb for recent
 600 years and smaller than 20 ppb prior to 1950. Black bars in ionic plots refer to the winter criteria.
 601 The black bars in the $\delta^{18}\text{O}$ plots refer to the respective mean value.

602

603 Examination of NH_4^+ and succinate minimum below 12 m depth showed that in contrast
 604 to what was seen in the Alps, the NH_4^+ winter level decreases significantly from near the
 605 surface to around 70 m w.e. depth (see Fig. 8). Therefore, the NH_4^+ winter and background
 606 criteria had been adjusted, using a winter (background) threshold of 50 ppb (30 ppb) from 52
 607 – 62 m w.e. of the core and 30 ppb (20 ppb) core down of 62 m w.e. In contrast, the succinate
 608 winter levels did not change and the 5 ppb criterion applied in recent times was also applied in
 609 deeper layers. Fig. 8 b, d, and f showed a comparison of NH_4^+ , succinate with the $\delta^{18}\text{O}$ record
 610 between 75 and 78 m w.e. (i.e. from 1931–1928). As observed for recent times, the winter
 611 criteria matches very good with winter deposition as deduced from the stable isotope content,

612 although the latter record tends to be already a bit smoothed compared to the uppermost firm
613 layers. As observed for the uppermost core section, it could not be excluded that the winter
614 criteria includes parts of the intermediate season, whereas the background criteria selects only
615 depositions arriving from the coldest precipitations.

616 Figure 9 shows the result of the dating of the Elbrus ice core. In addition to model
617 calculations which are detailed in section 3.4, the depth age scale obtained by annual layer
618 counting using the NH_4^+ – succinate criteria is reported down to 122 m w.e. Annual layer
619 counting was achieved as described above down to 85 m w.e. Further down, winter levels
620 became rather thin, due to annual layer thinning but probably also to upstream effects as
621 commonly encountered on such small-scale glaciers (Preunkert et al., 2000). Therefore, below
622 85 m w.e. ice core layers in which less than 3 samples have reached the winter criteria were
623 considered as winter seasons, and from 113 to 122 m w.e. winter layers were also assigned
624 when only one of the two criteria was fulfilled for at least one sample while the other one
625 showed only a relative minima (exceeding sometimes the fixed threshold). This could be
626 either due to the fact that winter sections become smaller than our depth resolution of 2–3 cm
627 applied core down of 90 m w.e., and/or be the result of an incomplete precipitation
628 preservation due to wind erosion upstream the borehole as already observed on small-scale
629 Alpine glacier sites (see e.g. Preunkert et al., 2000). In this latter case a systematic lack of
630 winter snow accumulation would occur in deeper ice core layers.



631

632 Figure 9. Depth (in m of ice equivalent)/age relation established for the Elbrus ice core by annual
 633 layer counting along the depth profile of ionic species (orange dots), and applying the ice flow
 634 models: Nye (blue line), Salamatin (green line). The inset represents the annual layers thickness
 635 (in m of ice equivalent) and the “Nye” least square fit (see text).

636

637 Dating based on annual layer counting of the chemical stratigraphy is in a fairly good
 638 agreement with the tritium 1963 time horizon that is located at the core depth of 50.7 m w.e.
 639 (dated at 1965 using the ammonium stratigraphy, Fig. 10a). In addition it fits very well with
 640 the dating achieved so far (i.e. core down to 106.7 m) on the base of the seasonal stratigraphy
 641 of the stable isotope profile. Whereas stable isotopes predict the year 1924 at a core depth of
 642 106.7 m, the chemical stratigraphy leads to estimate the year 1926 in this depth.

643 To anchor the depth age relation with further absolute time horizons, a first inspection
 644 of the sulfate profile was made in view to identify volcanic horizons as found in other
 645 northern hemisphere ice cores between 1912 (Katmai) and 1783 (Laki eruption) in Greenland
 646 (Legrand et al., 1997; Clausen et al., 1997) and at Colle Gnifetti (Bohleber 2008). However
 647 since the Elbrus is an in active volcanic crater, it is sometimes difficult to attribute a peak
 648 either to a well-known global eruption or to a local event. Furthermore, numerous sulphate
 649 peaks in the Elbrus ice core originate from terrestrial inputs as suggested by the presence of
 650 concomitant calcium peaks. So far, the Katmai eruption in 1912 could be clearly identified at

651 87.7 m w.e. (dated at 1911 using the ammonium stratigraphy) with several neighbored
652 samples showing relatively high sulfate levels (up to 1200 ppb, i.e. $25 \mu\text{Eq L}^{-1}$) compared to
653 those seen in sulphate peaks generally present in summer layers of the early 20th century.
654 Furthermore, as seen in Fig. 10b, in contrast to neighbored summer sulphate peaks located at
655 87.2, 87.4, 88.0, and 89.3 m w.e., that are alkaline (see Fig. 10b), the acidity of samples of the
656 87.7 m w.e. sulphate peak reaches $8 \mu\text{Eq L}^{-1}$ at the bottom part of the sulphate peak.
657 Furthermore, samples located of the top part of the 87.7 m w.e. sulfate peak remains neutral in
658 spite of a large presence of calcium (similar to those seen in neighbored summer sulphate
659 peaks). As seen in Figure 11 it appears that within one-year uncertainty this horizon is in
660 excellent agreement with our annual counting.

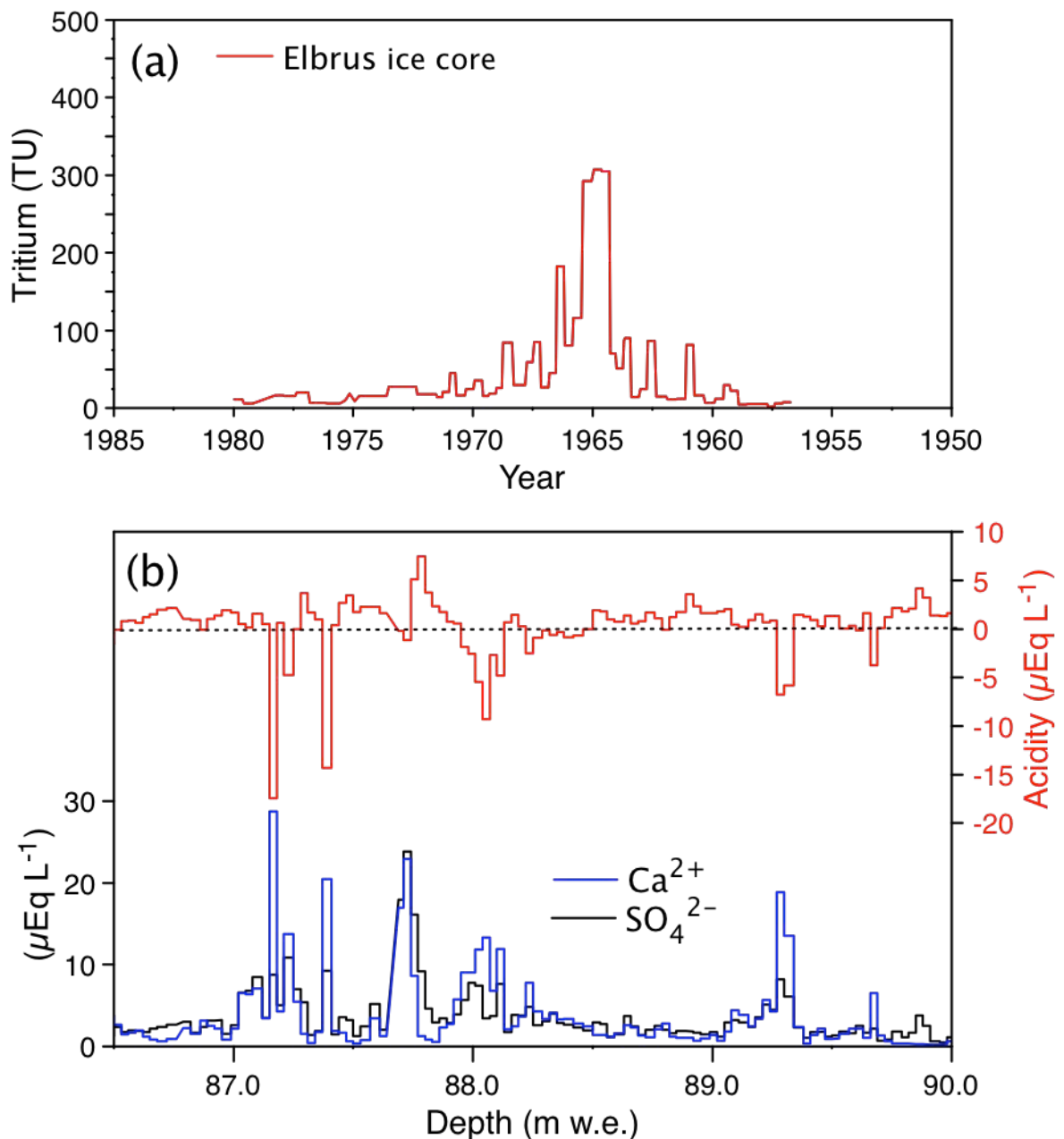
661 Below 88 m w.e., we were still able to easily proceed annual counting down to 113
662 (1860), whereas further down the dating become more uncertain (see the green line in Fig. 9).
663 Below 88 m w.e., 7 significant potential volcano horizons can be suspected on the basis of the
664 ionic balance and sulfate levels (not shown), from which however at least 1 are of local origin
665 (as suggested by small stones with size of up to 1–2 mm were found in the corresponding
666 layer). Nevertheless, a series of 3 narrow spikes was located at 118–120 m w.e. (dated at
667 around 1840–1833) among which two that are characterized by an increase of sulphate and
668 acidity (up to $7.8 \mu\text{Eq L}^{-1}$, not shown) may be related to the well-known eruptions observed in
669 Greenland in a time distance of 2 years around 1840 (one of them being possibly due to the
670 Coseguina eruption in 1835) (Legrand et al., 1997).

671 The depth / age relation was obtained from the annual layers counting along the depth
672 (Fig. 9). Despite high variability in the annual layers' thickness the data represents evident
673 thinning of the layers with depth related to the ice flow. Applying the form of the
674 thickness/age relationship as developed by Nye (Dansgaard & Johnsen, 1969) to the actual
675 annual layers data (see inset at Fig. 9) provides the mean accumulation over the whole time
676 period covered by the studied part of the ice core to be 1.583 m in ice equivalent. The “Nye”
677 curve, shown at Fig. 9, corresponds to the depth/age relationship from the Nye model with
678 such “best fit” (constant over time) accumulation rate and the glacier thickness as at the
679 drilling site. The blue line is the depth/age relation as suggested by Salamatin's model
680 (Salamatin et al., 2000) with the same “best fit to Nye” accumulation rate and the bed and
681 surface descriptions as at the drilling site.

682 Dating based on annual layer counting of the chemical stratigraphy is in a fairly good
683 agreement with the tritium 1963 time horizon that is located at the core depth of 50.7 m w.e.
684 (dated at 1965 using the ammonium stratigraphy, Fig. 10a). In addition it fits very well with

685 the dating achieved so far (i.e. core down to 106.7 m) on the base of the seasonal stratigraphy
686 of the stable isotope profile. Whereas stable isotopes predict the year 1924 at a core depth of
687 106.7 m, the chemical stratigraphy leads to estimate the year 1926 in this depth.

688 To anchor the depth age relation with further absolute time horizons, a first inspection
689 of the sulfate profile was made in view to identify volcanic horizons as found in other
690 northern hemisphere ice cores between 1912 (Katmai) and 1783 (Laki eruption) in Greenland
691 (Legrand et al., 1997; Clausen et al., 1997) and at Colle Gnifetti (Bohleber 2008). However
692 since the Elbrus is an in active volcanic crater, it is sometimes difficult to attribute a peak
693 either to a well-known global eruption or to a local event. Furthermore, numerous sulphate
694 peaks in the Elbrus ice core originate from terrestrial inputs as suggested by the presence of
695 concomitant calcium peaks. So far, the Katmai eruption in 1912 could be clearly identified at
696 87.7 m w.e. (dated at 1911 using the ammonium stratigraphy) with several neighbored
697 samples showing relatively high sulfate levels (up to 1200 ppb, i.e. $25 \mu\text{Eq L}^{-1}$) compared to
698 those seen in sulphate peaks generally present in summer layers of the early 20th century.
699 Furthermore, as seen in Fig. 10b, in contrast to neighbored summer sulphate peaks located at
700 87.2, 87.4, 88.0, and 89.3 m w.e., that are alkaline (see Fig. 10b), the acidity of samples of the
701 87.7 m w.e. sulphate peak reaches $8 \mu\text{Eq L}^{-1}$ at the bottom part of the sulphate peak.
702 Furthermore, samples located of the top part of the 87.7 m w.e. sulfate peak remains neutral in
703 spite of a large presence of calcium (similar to those seen in neighbored summer sulphate
704 peaks). As seen in Figure 9 it appears that within one-year uncertainty this horizon is in
705 excellent agreement with our annual counting.



706
 707 Figure 10. Absolute time horizons: (a) Tritium measurements made on Elbrus ice core samples
 708 (data were converted to 2009 with regard to the half-life time of tritium, $T_{1/2} = 12.32$ year). The
 709 dates reported in the tritium curve are derived from the ammonium stratigraphy. (b) Calculated
 710 acidity (top, see Sect. 3.3.1), calcium and sulfate (bottom) in ice layers located between 86.5 and
 711 90 m w.e.

712
 713 Below 88 m w.e., we were still able to easily proceed annual counting down to 113
 714 (1860), whereas further down the dating become more uncertain (see the green line in Fig. 9).
 715 Below 88 m w.e., 7 significant potential volcano horizons can be suspected on the basis of the
 716 ionic balance and sulfate levels (not shown), from which however at least 1 are of local origin
 717 (as suggested by small stones with size of up to 1–2 mm were found in the corresponding
 718 layer). Nevertheless, a series of 3 narrow spikes was located at 118–120 m w.e. (dated at

719 around 1840–1833) among which two that are characterized by an increase of sulphate and
720 acidity (up to $7.8 \mu\text{Eq L}^{-1}$, not shown) may be related to the well-known eruptions observed in
721 Greenland in a time distance of 2 years around 1840 (one of them being possibly due to the
722 Coseguina eruption in 1835) (Legrand et al., 1997).

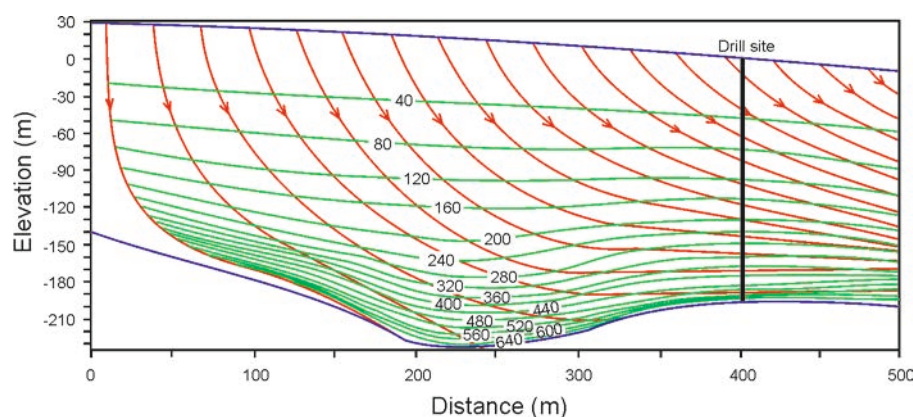
723

724 **3.4 Modelled ice flow and ice core dating**

725

726 From the thermodynamic point of view mountain glaciers filling volcano craters present a
727 special type. Relatively high crater depth and limited ice flux over the crater rims form flat
728 glacier surface result in small surface ice velocity. Intensive volcanic heat flux could result in
729 bottom melting and removal of the oldest basal layers. A simplified thermo mechanically
730 coupled model for simulating ice flow along a fixed flow tube and heat transfer in ice caps
731 filling volcanic craters has been developed by Salamatin et al. (2000). Model description and
732 ice-flow and heat-transfer equations are given in Salamatin et al. (2000). The model takes into
733 account surface and bedrock topography and snow-firn densification parameters (see section
734 3.3.2), the distribution of the relative bottom melt rate (see section 3.3.1) and normalized by
735 the present day accumulation rate. We calculated depth/age relationship for the Western
736 Elbrus Plateau on the basis of recent accumulation rate of 1200 mm w.e. The ice melt rate at
737 the glacier bedrock is negligible and comprises less than 10 mm w.e y^{-1} (see section 3.3.1) in
738 the deepest part at current accumulation rate limit. Figure 11 shows the cross section of the
739 Elbrus Western Plateau along a reference flow line. Predicted ice particle paths are shown by
740 arrowed lines, isochrones are designated by numbers, which specify the ice age in years.

741 The depth age relation calculated for the 2009 ice core is also given in Figure 9. It fits
742 well/fairly well with the dating on the annual layer counting. According to the modelling
743 results, the bottom ice age at the maximal depth is predicted to be about 660 years before
744 2009 AD and is close to the maximal age in the crater. A 2009 borehole was situated below
745 and the estimated bottom ice age does not exceed 350–400 years before 2009 AD.



746

747 Figure 11. Vertical transect of the Western Elbrus Plateau glacier along a reference flow line.
 748 Predicted ice-particle paths (lines with arrows) and isochrones are shown.

749

750 4. Conclusions

751

752 Paleoclimatological records for southern and eastern Europe are based on geomorphological,
 753 palinological, limnological, and dendrochronological data. Ice core records have not been
 754 taken into account as a source of paleoclimate and environmental information for this area
 755 due to rapid glacier mass exchange rate and significant surface melting, causing isotope and
 756 chemical profile smooth in the glacier depositions. The analysis of the ice core derived in
 757 2009 on the Mt. Elbrus at 5115 m provides new evidence for significant regional-scale
 758 multiproxy climatic implications. The negative ice temperature of the glacier at the drilling
 759 site secures an undisturbed incoming climate signal. The considerable snow accumulation rate
 760 of 1455 mm w.e. coupled with a great body of analyzed samples allow us to separate snow
 761 depositions from summer and winter precipitation. Annual layering was made on the basis of
 762 seasonal oscillations of NH_4^+ , succinic acid, and $\delta^{18}\text{O}$. Annual layer counting was secured
 763 down to 85 m w.e. The ice flow model shows that the near bedrock ice age at the maximal
 764 glacier depth of 255 m can reach more than 600 years. But the 2009 drilling site was situated
 765 downstream and where the bottom ice age does not exceed 350–400 years. An essential
 766 difference between reported depth-age scale constructed on the base of layer counting and
 767 modeled one demands the inspection of model algorithm and development of a reliable ice
 768 flow model. Annual layer counting was confirmed by the well-known reference horizons of
 769 the 1963 nuclear tests and the 1912 Katmai volcanic eruption. The comparison of Mt. Elbrus
 770 ice core records with ice core records from Alpine glaciers (Col du Dôme and Colle Gnifetti)
 771 will allow us to estimate the tendency of climatic changes over Europe for the last centuries,
 772 and to obtain high resolution multiproxy reconstructions of the dustiness of the atmosphere,

773 air temperature and precipitation oscillations, black carbon pollution, and atmospheric
774 circulation change.
775 Combining the different glacio-chemical features of the Western Elbrus Plateau detailed in
776 this study, we conclude that this high elevation glacier archive offers the possibility to extract
777 atmospheric relevant information from long-term ice core records. Ongoing works are
778 therefore dedicated to reconstructing several key aspects of the changing atmosphere of this
779 central European region, in particular for various components of aerosol (sulfate, ammonium,
780 terrigenous matter, and carbonaceous compounds or fractions) and species related to the
781 nitrogen cycle (nitrate).

782

783 *Acknowledgments.* The ice core recovery in 2009 was funded by the Russian Foundation for
784 Basic Research (RFBR) Grants 07-05-00410 and 09-05-10043. V. Mikhaleiko, S. Kutuzov, and
785 I. Lavrentiev acknowledge support of the Russian Academy of Sciences (Department of Earth
786 Sciences ONZ-12 Project) and RFBR Grant 14-05-00137. S. Sokratov acknowledges support of
787 the RSF (project 14-37-00038) in his contribution to the paper. The ongoing laboratory analyses
788 at LGGE and logistics were supported by the EU FP7 IP PEGASOS (FP7-ENV- 2010/265148),
789 the French ANR program PAPRIKA (ANR-09-CEP-005-02), the CNRS-DFG bilateral project
790 entitled “Secondary organic aerosol production in the lower free troposphere over western
791 Europe”, and the LEFE-CHAT program ESCCARGO. Stable water isotopic analyses were
792 supported by the RFBR Grant 14-05-31102 (A. Kozachek, A. Ekaykin, and V. Lipenkov, AARI)
793 and IAEA Research Contracts 16184/R0 (Stable water isotopes in the cryosphere of the Northern
794 Eurasia), and 16795 (Paleo-Climate Isotope Record from European Mt. Elbrus Ice Core). This
795 research work was conducted in the framework of the International Associated Laboratory (LIA)
796 “Climate and Environments from Ice Archives” 2012–2016 linking several Russian and French
797 laboratories and institutes.

798 **References**

799

- 800 Abich, H.: Geologische Beobachtungen auf Reisen im Kaukasus im Jahre 1873, Bulletin de la
801 Société impériale des naturalistes de Moscou, 48(2), 278–342 + 1 Karte, 1874a.
802 Abich, H.: Geologische Beobachtungen auf Reisen im Kaukasus im Jahre 1873 (Fortsetzung),
803 Bulletin de la Société impériale des naturalistes de Moscou, 48(3), 63–107, 1874b.
804 Abich, H.: Geologische Beobachtungen auf Reisen im Kaukasus im Jahre 1873 (Schluss),
805 Bulletin de la Société impériale des naturalistes de Moscou, 48(4), 243–272, 1874c.
806 AMAP: Snow, Water, Ice and Permafrost in the Arctic (SWIPA): Climate Change and the
807 Cryosphere, Arctic Monitoring and Assessment Programme (AMAP), Oslo, 538 pp., 2011.

808 Anisimov, O.A. and Zhil'tsova, E.L.: Climate change estimates for the regions of Russia in
809 the 20th century and in the beginning of the 21st century based on the observational data,
810 *Rus. Meteorol. Hydrol.*, 37(6), 421–429, doi:10.3103/S1068373912060106, 2012.

811 Arkhipov, S.M., Mikhaleiko, V.N., Thompson, L.G., Zagorodnov, V.S., Kunakhovich, M.G.,
812 Smirnov, K.E., Makarov, A.V., and Kuznetsov, M.P.: Stratigrafiya deyatelnogo sloya
813 lednikovogo kupola Vetreniy na ostrove Graham Bell, Zemlya Frantsa Iosifa (Stratigraphy of
814 the active layer of the Vetreny Ice Cap, Graham Bell Island, Franz Josef Land), *Materialy*
815 *glyatsiologicheskikh issledovaniy (Data Glaciol. Stud.)*, (90), 169–186, 2001 (in Russian
816 with English summary).

817 ASTER GDEM Validation Team: ASTER Global DEM Validation Summary Report, Sioux
818 Falls, USA, 28 pp., 2009.

819 Baranov, S. and Pokrovskaya, T.: Rabota meteorologicheskoi gruppy EKNE 1935
820 (Investigations of the Meteorological team of the Elbrus Complex Scientific Expedition),
821 in: *Trudy Elbrusskoi ekspeditsii Akademii nauk SSSR i VIEM 1934 i 1935 gg.*; *Trudy*
822 *komissii po izucheniyu stratosfery*, t. 2 (Elbrus expedition of the Academy of Sciences and
823 of the Institute of Experimental Medicine of the USSR, 1934 and 1935; Proceedings of the
824 commission of the stratosphere investigations, v. 2), resp. ed.: Vavilov, S.I., Academy of
825 Sciences Press, Moscow, Leningrad, 199–209, 1936 (in Russian with English summary).

826 Barbante, C., Schwikowski, M., Ring, T., Gäggeler, H.W., Schotterer, U., Tobler, L., Van de
827 Velde, K., Ferrari, C., Cozzi, G., Turetta, A., Rosman, K., Bolshov, M., Capodaglio, G.,
828 Cescon, P., and Bourton, C.: Historical record of European emissions of heavy metals to
829 the atmosphere since the 1650s from Alpine snow/ice cores drilled near Monte Rosa,
830 *Environ. Sci. Technol.*, 38(15), 4085–4090, doi:10.1021/es049759r, 2004.

831 Bazhev, A.B. and Bazheva, V.Ya.: Stroenie firново-ledyanoy tolschi na Elbruse (Structure and
832 firn-ice layer at the south slope of Elbrus), *Materialy glyatsiologicheskikh issledovaniy (Data*
833 *Glaciol. Stud.)*, (10), 94–100, 1964 (in Russian with English summary).

834 Bazhev, A.B., Rototaeva, O., Heitzenberg, J., Stenberg, M., and Pinglot, J.F.: Physical and
835 chemical studies in the region of the southern slope of Mount Elbrus, Caucasus, *J. Glaciol.*,
836 44(147), 214–222, 1998.

837 Bender, M. Sowers, T., and Brook, E.: Gases in ice cores, *P. Natl. Acad. Sci. USA*, 94(16),
838 8343–8349, doi:10.1073/pnas.94.16.8343, 1997.

839 Berikashvili, V.Sh., Vasilenko, E.V., Macheret, Yu.Ya., and Sokolov, V.G.: Odnoimpul'sniy
840 radar dlya zondirovaniya lednikov s opticheskim kanalom sinkhronizatsii (Monopulse
841 radar for glacier sounding with optical channel for synchronization and digital signal

842 processing), Radiotekhnika (Radio technics), (9), 52–57, 2006 (in Russian with English
843 summary).

844 Bohleber, P.: Age distribution and $\delta^{18}\text{O}$ variability in a low accumulation Alpine ice core:
845 Perspective for paleoclimate studies, Diploma thesis, Fakultät für Physik und Astronomie,
846 Ruprecht-Karls-Universität, Heidelberg, 147 pp., 2008.

847 Clausen, H.B., Hammer, C.U., Hvidberg C.D., Dahl-Jensen, D., Kipfstuhl, J., and Legrand, M.:
848 A comparison of the volcanic records over the past 4000 years from the Greenland Ice Core
849 Project and Dye 3 Greenland ice cores, *J. Geophys. Res.*, 102(C12), 26707–26723,
850 doi:10.1029/97JC00587, 1997.

851 Dansgaard, W., Johnsen, S.J. A flow model and a time scale for the ice core from Camp Century,
852 Greenland, *J. Glaciol.*, 8(53), 215–223, 1969.

853 Dolgova E.A., Matskovskiy V.V., Solomina O.N., Rototarva O.V., Nosenko G.A., and
854 Khmelevskoy I.F.: Rekonstruktsiya balansa massy lednika Garabashi (1800–2005) po
855 dendrokronologicheskim dannim (Reconstructing mass balance of Grabashi Glacier
856 (1800–2005) using dendrochronological data), *Led i Sneg (Ice and Snow)*, 53(1), 34–42,
857 doi:10.15356/2076-6734-2013-1-34-42, 2013 (in Russian with English summary).

858 Dyurgerov, M.B. and Popovnin, V.V.: Rekonstruktsiya balansa massy, prostranstvennogo
859 polozheniya i zhidkogo stoka lednika Dzhankuat so vtoroi poloviny 19 veka
860 (Reconstruction of mass balance, spatial position, and liquid discharge of Dzhankuat
861 Glacier since the second half of the 19th century), *Materialy glyatsiologicheskikh*
862 *issledovaniy (Data Glaciol. Stud.)*, (40), 111–126, 1988 (in Russian with English summary).

863 Eichler, A., Tinner, W., Brusch, S., Olivier, S., Papina, T., and Schwikowski, M.: An ice-core
864 based history of Siberian forest fires since AD 1250, *Quaternary Sci. Rev.*, 30(9–10),
865 1027–1034, doi:10.1016/j.quascirev.2011.02.007, 2011.

866 Fagerli H., Legrand, M., Preunkert, S., Vestreng, V., Simpson, D., and Cerquera, M.:
867 Modeling historical long-term trends of sulfate, ammonium, and elemental carbon over
868 Europe: A comparison with ice core records in the Alps. *J. Geophys. Res.*, 112(D23),
869 D23S13: 1–16, doi:10.1029/2006JD008044, 2007.

870 Ginot, P., Schotterer, U., Stichler, W., Godoi, M. A., Francou, B., and Schwikowski, M.:
871 Influence of the Tungurahua eruption on the ice core records of Chimborazo, Ecuador, *The*
872 *Cryosphere*, 4(4), 561–568, doi:10.5194/tc-4-561-2010, 2010.

873 Golubev, G.N., Dyurgerov, M.B., Markin, V.A., Berry, B.L., Sukhanov, L.A., Zolotarev,
874 E.A., Danilina, A.V., and Arutunov, Yu.G.: *Lednik Dzhankuat (Tsentralniy Kavkaz)*
875 (Water-ice and heat balances of Jankuat Glacier (Central Caucasus)), edited by: Byarski,

- 876 I, Ya., Hydrometeoizdat Press, Leningrad, 184 pp., 1978 (in Russian with English
877 summary).
- 878 Golubev, V.N., Mikhailenko, V.N., Serebrennikov, A.V., and Gvozdk, O.A.: Strukturnye
879 issledovaniya ledyanogo kerna Dzhantuganskogo firnovogo plato na Tsentral'nom
880 Kavkaze (Structural studies of the ice core obtained from the Dzhantugan Firn Plateau in the
881 Central Caucasus), *Materialy glyatsiologicheskikh issledovaniy (Data Glaciol. Stud.)*, (64),
882 25–33, 1988 (in Russian with English summary).
- 883 Hörhold, M.W., Kipfstuhl, S., Wilhelms, F., Freitag, J., and Frenzel, A.: The densification of
884 layered polar firn, *J. Geophys. Res.*, 116(F1), F01001: 1–15, doi:10.1029/2009JF001630,
885 2011.
- 886 Hou, S., Chappellaz, J., Raynaud, D., Masson-Delmotte, V., Jouzel, J., Bousquet P., and
887 Hauglustaine D.: A new Himalayan ice core CH₄ record: possible hints at the preindustrial
888 latitudinal gradient, *Clim. Past*, 9(6), 2549–2554, doi:10.5194/cp-9-2549-2013, 2013.
- 889 Johnsen, S., Clausen, H.B., Cuffey, K.M., Hoffmann, G., Schwander, J., and Creyts, T.:
890 Diffusion of stable isotopes in polar firn and ice: the isotope effect in firn diffusion, in:
891 *Physics of Ice Core Records*, edited by Hondoh, T., Hokkaido University Press, Sapporo,
892 121–140, doi:10.7916/D8KW5D4X, 2000.
- 893 Kawamura, K., Izawa, Y., Mochida, M., and Shiraiwa, T.: Ice core records of biomass
894 burning tracers (levoglucosan and de-hydroabietic, vanillic and p-hydroxybenzoic acids)
895 and total organic carbon for past 300 years in the Kamchatka Peninsula, Northeast Asia,
896 *Geochim. Cosmochim. Ac.*, 99, 317–329, doi:10.1016/j.gca.2012.08.006, 2012.
- 897 Kerimov, A.M., Rototaeva, O.V., and Khmelevskoy, I.F.: Raspredelenie tyazhelykh metallov
898 v poverkhnostnykh sloyakh snezhno-firnovoi tolshchi na yuzhnom sklone Elbrusa
899 (Distribution of heavy metals in the surface layers of snow-firn mass on the southern slope
900 of Mount Elbrus), *Led i Sneg (Ice and Snow)*, 51(2), 24–34, doi:10.15356/2076-6734-
901 2011-2-24-34, 2011 (in Russian with English summary).
- 902 Kotlyakov, V.M., Arkhipov, S.M., Henderson, K.A., and Nagornov, O.V.: Deep drilling of
903 glaciers in Eurasian Arctic as a source of paleoclimatic records, *Quaternary Sci. Rev.*,
904 23(11–13), 1371–1390, doi:10.1016/j.quascirev.2003.12.013, 2004.
- 905 Kovalev P.V.: Sovremennoe oledenenie basseina reki Baksan (Recent glaciation of the
906 Baksan River basin), in: *Materialy Kavkazskoi ekspeditsii (po programme*
907 *Mezhdunarodnogo geofizicheskogo goda) (Proc. of the Caucasus expedition (by the*
908 *programme of the International Geophysical Year))*, v. 2, edited by: Dubinskii G.P.,
909 Khar'kov University, Khar'kov, 3–106, 1961 (in Russian).

- 910 Krenke, A.N., Menshutin, V.V., Voloshina, A.P., Panov, V.D., Bazhev, A.B., Bazheva, V.Ja.,
911 Balaeva, V.A., Vinogradov, O.N., Voronina, L.S., Garelik, I.S., Davidovich, N.V.,
912 Dubinskaya, N.M., Macheret, Yu.Ya., Moiseeva, G.P., Psareva, T.V., Tyulina, T.Yu.,
913 Freidlin, V.S., Khmelevskoy, I.F., Chernova, L.P., and Shadrina, O.V.: *Lednik Marukh*
914 (*Zapadniy Kavkaz*) (*Marukh Glacier (Western Caucasus)*), edited by: Kotlyakov, V.M.,
915 Hydrometeoizdat Press, Leningrad, 254, 1988 (in Russian with English summary).
- 916 Kutuzov S., Lavrentiev, I. I., Macheret, Yu, Ya., and Petrakov, D. A.: *Izmenenie lednika*
917 *Marukh s 1945 po 2011* (*Changes of Marukh Glacier from 1945 to 2011*), *Led i Sneg* (*Ice*
918 *and Snow*), 52(1), 123–127, doi:10.15356/2076-6734-2012-1-123-127, 2012 (in Russian
919 with English summary)
- 920 Kutuzov S.S., Lavrentiev I.I., Vasilenko E.V., Macheret Y.Y., Petrakov D.A., and Popov
921 G.V.: *Otsenka obiyema lednikov Bolshogo Kavkaza po dannym radiozondirovaniya i*
922 *modelirovaniya* (*Estimation of the Greater Caucasus glaciers volume, using radio-echo*
923 *sounding data and modelling*), *Kriosfera Zemli* (*Earth’s Cryosphere*), 19(1), 78–88, 2015
924 (in Russian with English summary)
- 925 Kutuzov, S., Shahgedanova, M., Mikhalenko, V., Lavrentiev, I, and Kemp, S.: *Desert dust*
926 *deposition on Mt. Elbrus, Caucasus Mountains, Russia in 2009–2012 as recorded in snow*
927 *and shallow ice core: high-resolution “provenancing”, transport patterns, physical*
928 *properties and soluble ionic composition*, *The Cryosphere*, 7(5), 1481–1498,
929 doi:10.5194/tc-7-1481-2013, 2013.
- 930 Laverov, N.P., Dobretsov, N.L., Bogatikov, O.A., Bondur, V.G., Gurbanov, A.G.,
931 Karamurзов, B.S., Kovalenko, V.I., Melekestsev, I.V., Nechaev, Yu.V., Ponomareva,
932 V.V., Rogozhin, E.A., Sobisevich, A.L., Sobisevich, L.E., Fodotov, S.A., Khrenov, A.P.,
933 and Yarmolyuk, V.V.: *Noveyshiy i sovremenniy vulkanizm na territorii Rossii* (*Modern*
934 *and Holocene volcanism in Russia*), Nauka, Moscow, 604 pp., 2005 (in Russian with
935 English summary).
- 936 Lavrentiev, I.I., Mikhalenko, V.N., and Kutuzov, S.S.: *Tolshchina l’da i podlednyi rel’ef*
937 *Zapadnogo lednikovogo plato Elbrusa* (*Ice thickness and subglacial relief of the Western*
938 *Ice Plateau of Elbrus*), *Led i Sneg* (*Ice and Snow*), 50(2), 12–18, doi:10.15356/2076-6734-
939 2010-2-12-18, 2010 (in Russian with English summary).
- 940 Legrand M., C. Hammer, M. De Angelis, J. Savarino, R. Delmas, H. Clausen, and S.J. Johnson,
941 Sulphur containing species (MSA and SO₄) over the last climatic cycle in the GRIP (central
942 Greenland) ice core, *J. Geophys. Res.*, 102(C12), 26663–26679, doi:10.1029/97JC01436,
943 1997.
- 944 Legrand, M. and Mayewski, P.: *Glaciochemistry of polar ice cores: A review*, *Rev. Geophys.*,

945 35(3), 219–243, doi:10.1029/96RG03527, 1997.

946 Legrand, M., Preunkert, S., Schock, M., Cerqueira, M., Kasper-Giebl, A., Afonso, J., Pio, C.,
947 Gelencsér, A. and Dombrowski-Etchevers, I.: Major 20th century changes of carbonaceous
948 aerosol components (EC, WinOC, DOC, HULIS, carboxylic acids, and cellulose) derived
949 from Alpine ice cores, *J. Geophys. Res.*, 112(D23), D23S11, doi:10.1029/2006JD008080,
950 2007a.

951 Legrand, M., S. Preunkert, Oliveira, T., Pio, C.A., Hammer, S., Gelencsér, A., Kasper-Giebl, A.,
952 and Laj, P.: Origin of C₂–C₅ dicarboxylic acids in the European atmosphere inferred from
953 year-round aerosol study conducted at a west-east transect, *J. Geophys. Res.*, 112(D23),
954 D23S07, doi:10.1029/2006JD008019, 2007b.

955 Ligtenberg, S.R.M., Helsen, M.M., and van den Broeke, M.R.: An improved semi-empirical
956 model for the densification of Antarctic firn, *The Cryosphere*, 5(4), 809–819,
957 doi:10.5194/tc-5-809-2011, 2011.

958 Looyenga, M.: Dielectric constant of heterogeneous mixtures, *Physica*, 31(3), 401–406,
959 doi:10.1016/0031-8914(65)90045-5, 1965.

960 Macheret, Yu.Ya.: Radiozondirovanie lednikov (Radio-echo sounding of glaciers), Scientific
961 World Publishers, Moscow, 392 pp., 2006 (in Russian with English summary).

962 Maeno, N. and Ebinuma, T.: Pressure sintering of ice and its implication to the densification
963 of snow at polar glaciers and ice sheets, *J. Phys. Chem.*, 87(21), 4103–4110,
964 doi:10.1021/j100244a023, 1983.

965 Matyukhin, G.D.: Klimaticheskie dannye po vysotnym poyasam yuzhnogo sklona Elbrusa
966 (Climatic data for the southern slope of Elbrus), in: *Informatsionnyi sbornik o rabotakh po*
967 *Mezhdunarodnomu geofizicheskomu godu* (Information collection on the investigations in
968 *International Geophysical Year*), 5, Faculty of Geography, Moscow State University,
969 Moscow, 130–194, 1960 (in Russian).

970 Mätzler, C. and Wegmüller, U.: Dielectric properties of fresh-water ice at microwave
971 frequencies, *J. Phys. D Appl. Phys.*, 20(12), 1623–1630, doi:10.1088/0022-
972 3727/20/12/013, 1987.

973 Mikhailenko, V.N., Kuruzov, S.S., Lavrentiev, I.I., Kunakhovich, M.G., and Thompson, L.G.:
974 Issledovanie zapadnogo lednikovogo plato Elbrusa: rezul'taty i perspektivy (Western
975 Elbrus Plateau studies: results and perspectives), *Materialy glyatsiologicheskikh issledovaniy*
976 *(Data Glaciol. Stud.)*, (99), 185–190, 2005 (in Russian with English summary)

977 Mikhailenko, V.N.: Glubinnoe stroenie lednikov tropicheskikh i umerennikh shirot (Inner
978 structure of glaciers in non-polar regions), LKI Publishers, Moscow, 320 pp., 2008 (in
979 Russian with English summary).

- 980 Mikhalenko, V.N.: Glubokoe burenie l'la bliz vershiny Elbrusa (Deep ice core drilling near
981 summit of Mt. Elbrus), *Led i Sneg (Ice and Snow)*, 50(1), 123–126, doi:10.15356/2076-
982 6734-2010-1-123-126, 2010 (in Russian with English summary).
- 983 Mushketov, I.V.: Geologicheskaya poezdka na Kavkaz v 1881 (Geological excursion to the
984 Caucasus in 1881), *Izvestiya Imperatorskogo Russkogo geograficheskogo obshchestva*
985 (Proc. Rus. Geogr. Soc.), 18(2), 106–119, 1882 (in Russian).
- 986 Nosenko, G.A., Khromova, T.E., Rototaeva, O.V., and Shahgedanova, M.: Reaktsiya
987 lednikov Tsentralnogo Kavkaza v 2001–2010 na izmeneniya temperatury i kolichestva
988 osadkov (Glacier reaction to temperature and precipitation change in Central Caucasus),
989 2001–2010, *Led i Sneg (Ice and Snow)*, 53(1), 26–33, doi:10.15356/2076-6734-2013-1-26-
990 33, 2013 (in Russian with English summary).
- 991 Pastukhov, A.V.: Poseshchenie Elbrusa 13 iyulya 1890 (Ascending to Elbrus on 13 July,
992 1890), *Zapiski Kavkazskogo otdela Imperatorskogo Russkogo geograficheskogo*
993 *obshchestva (Mem. Cauc. branch Imperial Rus. Geogr. Soc.)*, 15, 22–37, 1893 (in
994 Russian).
- 995 Podozerski, K.I.: Ledniki Kavkazskogo khrebt (Glaciers of the Caucasus Range), *Zapiski*
996 *Kavkazskogo otdela Imperatorskogo Russkogo geograficheskogo obshchestva (Mem. Cauc.*
997 *branch Imperial Rus. Geogr. Soc.)*, 29(1), 200 pp., 1911 (in Russian).
- 998 Preunkert, S. and Legrand, M.: Towards a quasi-complete reconstruction of past atmospheric
999 aerosol load and composition (organic and inorganic) over Europe since 1920 inferred
1000 from Alpine ice cores, *Clim. Past*, 9(4), 1403–1416, doi:10.5194/cp-9-1403-2013, 2013.
- 1001 Preunkert, S., Wagenbach, D., Legrand, M., and Vincent, C.: Col du Dôme (Mt Blanc Massif,
1002 French Alps) suitability for ice-core studies in relation with past atmospheric chemistry
1003 over Europe, *Tellus*, 52B(3), 993–1012, doi:10.1034/j.1600-0889.2000.d01-8.x, 2000.
- 1004 Psareva, T.V.: Preobrazovanie snezhno-firnvoi tolshechi i tipy l'doobrazovaniya na Elbruse
1005 (Transformation of snow-firn thickness and types of ice formation on Elbrus), *Materialy*
1006 *glyatsiologicheskikh issledovaniy (Data Glaciol. Stud.)*, (10), 79–86, 1964 (in Russian with
1007 English summary).
- 1008 Rototaeva, O.V. and Tarasova, L.N.: Rekonstruktsiya balansa massi lednika Garabashi za
1009 poslednee stoletie (Reconstruction of the Garabashi Glacier mass balance in the last century),
1010 *Materialy glyatsiologicheskikh issledovaniy (Data Glaciol. Stud.)*, (88), 16–26, 2000 (in
1011 Russian with English summary).
- 1012 Rototaeva, O.V., Nosenko, G.A., Tarasova, L.N., and Khmelevskoy, I.F.: obshchaya
1013 kharakteristika oledeneniya severnogo sklona Bolshogo Kavkaza (General characteristics of
1014 glacierization of the north slope of the Greater Caucasus), in: *Sovremennoe oledenenie*

- 1015 Severnoi i Tsentralnoi Evrazii (Glaciation in North and Central Eurasia at present time),
1016 edited by: Kotlakov, V.M., Nauka Press, Moscow, 141–144, 2006 (in Russian).
- 1017 Salamatin, A.N., Lipenkov, V.Ya., Barnola, J.-M., Hori, A., Duval, P., and Hondoh T.: Snow/firn
1018 densification in polar ice sheets, in: Physics of Ice Core Records II: Papers collected after the
1019 2nd International Workshop on Physics of Ice Core Records, held in Sapporo, Japan, 2–6
1020 February 2007 (Low Temperature Science; 68(Suppl.)), edited by: Hondoh, T., Sapporo,
1021 Institute of Low Temperature Science, Hokkaido University, 195–222, 2009.
- 1022 Salamatin, A.N., Murav'yev, Y.D., Shiraiwa, T., and Matsuoka, K.: Modelling dynamics of
1023 glaciers in volcanic craters, *J. Glaciol.*, 46(153), 177–187, doi:10.3189/172756500781832990,
1024 2000.
- 1025 Salamatin, A.N., Shiraiwa, T., Muravyev, Y.D., Kameda, T., Silantiyeva, E., and Ziganshin, M.:
1026 Dynamics and borehole temperature memory of Gorshkov Ice Cap on the summit of
1027 Ushkovsky Volcano, Kamchatka Peninsula, Proceedings of the International Symposium on the
1028 Atmosphere-Ocean-Cryosphere Interaction in the Sea of Okhotsk and the Surrounding
1029 Environments held at Institute of Low Temperature Science, Hokkaido University, Sapporo,
1030 Japan, December 12–15, 2000, 120–121, 2001.
- 1031 Sato, T., Shiraiwa, T., Greve, R., Seddik, H., Edelman, E., and Zwinger, T.: Accumulation
1032 reconstruction and water isotope analysis for 1736–1997 of an ice core from the
1033 Ushkovsky volcano, Kamchatka, and their relationships to North Pacific climate records,
1034 *Clim. Past*, 10(1), 393–404, doi:10.5194/cp-10-393-2014, 2014.
- 1035 Schwikowski, M.: Reconstruction of European air pollution from Alpine ice cores, in: Earth
1036 Paleoenvironments: Records Preserved in Mid- and Low-Latitude Glaciers, edited by:
1037 DeWayne Cecil, L., Green, J.R., Thompson, L.G., *Developments in Paleoenvironmental*
1038 *Research*, 9, Kluwer Academic Publishers, 95–119, doi:10.1007/1-4020-2146-1_6, 2004.
- 1039 Serebryanny, L.R., Golodkovskaya, N.A., Orlov, A.V., Malyasova, E.S., and Il'ves, E.O.:
1040 Kolebaniya lednikov i protsessy morenolakopleniya na Tsentralnom Kavkaze (Glacier
1041 variations and moraine accumulation: processes in Central Caucasus), Nauka, Moscow,
1042 216 pp., 1984 (in Russian with English summary).
- 1043 Shahgedanova M., Nosenko G., Kutuzov S., Rototaeva O., and Khromova T.: Deglaciation of
1044 the Caucasus Mountains, Russia/Georgia, in the 21st century observed with ASTER
1045 satellite imagery and aerial photography, *The Cryosphere*, 8(6), 2367–2379,
1046 doi:10.5194/tc-8-2367-2014, 2014.
- 1047 Shahgedanova, M., Kutuzov, S., White, K., and Nosenko, G.: Using the significant dust
1048 deposition event on the glaciers of Mt. Elbrus, Caucasus Mountains, Russia on 5 May 2009

1049 to develop a method for dating and provenancing of desert dust events recorded in snow
1050 pack, *Atmos. Chem. Phys.*, 13(4), 1797–1808, doi:10.5194/acp-13-1797-2013, 2013.

1051 Solomina O.N., Kalugin, I.A., Aleksandrin, M.Yu., Bushueva, I.S., Darin, A.V., Dolgova,
1052 E.A., Jomelli, V., Ivanov, M.N., Matskovsky, V.V., Ovchinnikov, D.V., Pavlova, I.O.,
1053 Razumovsky, L.V., and Chepurnaya, A.A.: Burenie osadkov ozera Kara-Kel' (dolina reki
1054 Teberdy) I perspektivy rekonstruktsii istorii oledneniya i klamata golotsena na Kavkaze
1055 (Coring of Karakel' Lake sediments (Teberda River valley) and prospects for
1056 reconstruction of glaciation and Holocene climate history in the Caucasus), *Led i Sneg (Ice
1057 and Snow)*, 53(2), 102–111, doi:10.15356/2076-6734-2013-2-102-111, 2013 (in Russian
1058 with English summary).

1059 Solomina, O.N., Dolgova, E.A., and Maximova, O.E.: Rekonstruktsiya
1060 gidrometeorologicheskikh uslovii poslednikh stoletii na severnom Kavkaze, v Krymu i na
1061 Tyan' Shane po dendrokronologicheskim dannym (Tree-ring based hydrometeorological
1062 reconstructions in the Crimea, the Caucasus and Tien-Shan), Nestor History Press,
1063 Moscow, St. Petersburg, 232 pp., 2012 (in Russian with English summary).

1064 Stokes, C.R., Gurney, S.D., Shahgedanova, M, and Popovnin, V.: Late-20th-century changes
1065 in glacier extent in the Caucasus Mountains, Russia/Georgia, *J. Glaciol.*, 52(176), 99–109,
1066 doi:10.3189/172756506781828827, 2006.

1067 Takeuchi, N., Takahashi, A., Uetake, J., Yamazaki, T., Aizen, V. B., Joswiak, D., Surazakov,
1068 A. and Nikitin, S.: A report on ice core drilling on the western plateau of Mt. Belukha in
1069 the Russian Altai Mountains in 2003, *Polar Meteorol. Glaciol.*, 18, 121–133, 2004.

1070 Thompson, L.G.: Understanding Global Climate Change: Paleoclimate Perspective from the
1071 World's Highest Mountains, *Proc. Amer. Phil. Soc.*, 154(2), 133–157, 2010.

1072 Troshkina, E.S.: Stratigrafiya snazhno-firnovogo pokrova v oblasti pitaniya (Snow and firn
1073 stratigraphy in the accumulation zone of the Mt. Elbrus), in: *Olednenie Elbrusa (Elbrus
1074 Glaciation)*, edited by Tushinski, G.K., Moscow University Press, Moscow, 213–222, 1968
1075 (in Russian).

1076 Tushinskii, G.K. (ed.): *Olednenie Elbrusa (Glaciation of the El'brus Mountain)*, Moscow
1077 University Press, Moscow, 346 pp., 1968 (in Russian)

1078 Vasilenko, E.V., Glazovsky, A.F., Macheret, Yu.Ya., Navarro, F., Sokolov, V.G., and
1079 Shiraiwa, T.: Georadar VIRL dlya zondirovaniya lednikov (Georadar VIRL for glacier
1080 sounding), *Materialy glyatsiologicheskikh issledovaniy (Data Glaciol. Stud.)*, (94), 225–234,
1081 2003 (in Russian with English summary).

1082 Vasilenko, E.V., Sokolov, V.A., Macheret, Y., Glazovsky, A.F., Cuadrado, M.L., and
1083 Navarro, F.J.: A digital recording system for radioglaciological studies, *Bull. R. Soc. N. Z.*,
1084 35, 611–617, 2002.

1085 Vaughan, D.G., Comiso, J.C., Allison, I., Carrasco, J., Kaser, G., Kwok, R., Mote, P., Murray,
1086 T., Paul, F., Ren, J., Rignot, E., Solomina, O., Steffen, K., and Zhang, T.: Observations:
1087 Cryosphere, in: *Climate Change 2013: The Physical Science Basis. Contribution of*
1088 *Working Group I to the Fifth Assessment Report of the Intergovernmental Panel on*
1089 *Climate Change*, edited by: Stocker, T.F., Qin, D., Plattner, G.-K., Tignor, M., Allen, S.K.,
1090 Boschung, J., Nauels, A., Xia, Y., Bex, V., and Midgley, P.M., Cambridge University
1091 Press, Cambridge, United Kingdom and New York, NY, USA, 317–382, 2013.

1092 Vimeux, F., Ginot, P., Schwikowski, M., Vuille, M., Hoffmann, G., Thompson, L. G., and
1093 Schotterer, U.: Climate variability during the last 1000 years inferred from Andean ice
1094 cores: A review of methodology and recent results, *Palaeogeogr., Palaeoclimatol.,*
1095 *Palaeoecol.*, 281(3–4), 229–241, doi:10.1016/j.palaeo.2008.03.054, 2009.

1096 Volodicheva, N.: The Caucasus, in: *The Physical geography of Northern Eurasia*, edited by:
1097 Shahgedanova, M., Oxford University Press, Oxford, 350–376, 2002.

1098 Werner, M., Mikolajewicz, U., Heimann, M., and Hoffmann, G.: Borehole versus isotope
1099 temperatures on Greenland: Seasonality does matter, *Geophys. Res. Lett.*, 27(5), 723–726,
1100 doi:10.1029/1999GL006075, 2000.

1101 Zagorodnov, V.S., Arkhipov, S.M., Bazhev, A.B., Vostokova, T.A., Korolev, P.A.,
1102 Rototaeva, O.V., Sinkevich, S.A., and Khmelevskoy, I.F.: Stroenie, sostav i
1103 gidrotermichaskiy rezhim lednika Garabashi na Elbruse (Structure, state and hydrothermal
1104 regime of the Garabashi Glacier), the Elbrus area, *Materialy glyatsiologicheskikh*
1105 *issledovaniy (Data Glaciol. Stud.)*, (73), 109–117, 1992 (in Russian with English summary).

1106 Zagorodnov, V.S., Nagornov, O.V., and Thompson, L.G.: 2006. Influence of air temperature
1107 on a glacier's active-layer temperature. *Ann. Glaciol.*, 43, 285–287,
1108 doi:10.3189/172756406781812203, 2006.

1109 Zolotarev, E.A.: Evolutsiya oledeneniya Elbrusa: katrografo-aerokosmicheskie tekhnologii
1110 glyatsiologicheskogo monitoringa (Evolution of Elbrus glaciers: Cartographic-aerospace
1111 technologies of glacier monitoring), *Nauchnyi Mir*, Moscow, 238 pp., 2009 (in Russian).

1112 Zolotarev, E.A. and Kharkovets, E.G.: Oledenenie Elbrusa v kontse XX veka: tsifrovaya
1113 ortofotokarta Elbrusa na 1997 (Glaciation of Elbrus at the end of XX century (digital
1114 orthophotomap of Elbrus for 1997)), *Materialy glyatsiologicheskikh issledovaniy (Data*
1115 *Glaciol. Stud.)*, (89), 175–191, 2000 (in Russian with English summary).

- 1116 Zolotarev, E.A. and Kharkovets, E.G.: Evolutsiya oledeneniya Elbrusa posle malogo
1117 lednikovogo perioda (Development of glaciers of Mount Elbrus after the Little Ice Age),
1118 Led i Sneg (Ice and Snow), 52(2), 15–22, doi:10.15356/2076-6734-2012-2-15-22, 2012 (in
1119 Russian with English summary).